$t\bar{t}$+quarks production in ATLAS and CMS

Seth Moortgat
Interuniversity Institute for High Energies (IIHE)
Vrije Universiteit Brussel
seth.moortgat@cern.ch

Mahsana Haleem
JMU Wuerzburg
Mahsana.Ahsan@cern.ch

On behalf of the CMS and ATLAS Collaborations

LHCtopWG meeting (virtual), 23-11-2020

Overview

With a detector in between, quarks are observed as jets!

$t\bar{t}$ + ~~quarks~~

$t\bar{t}$ + jets

"what we see in the detector"

ATLAS

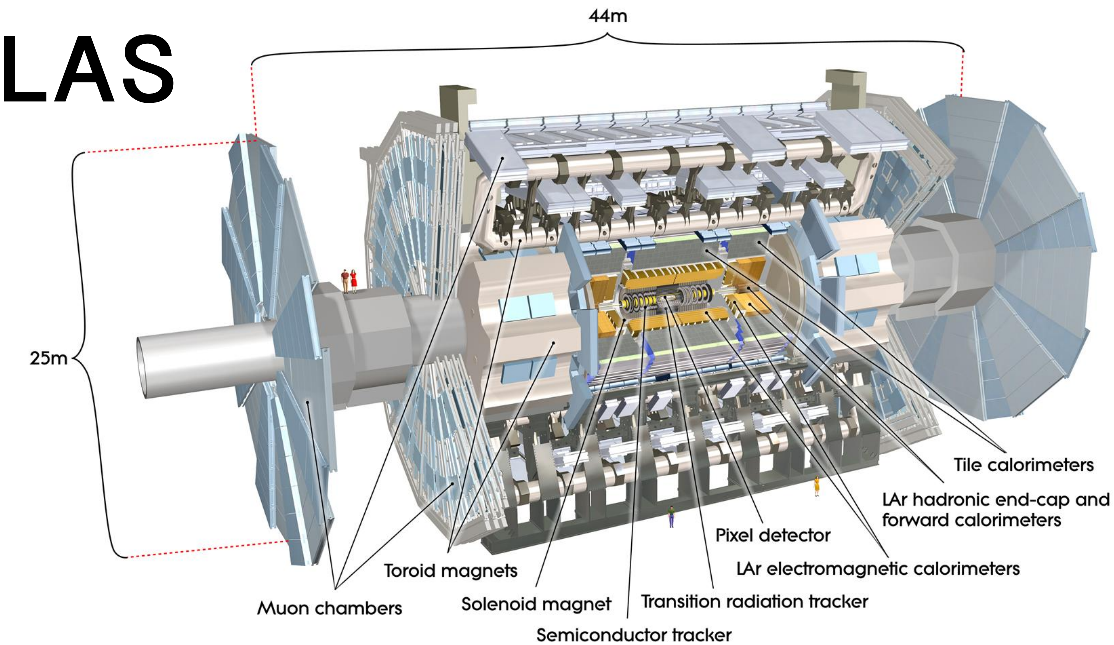

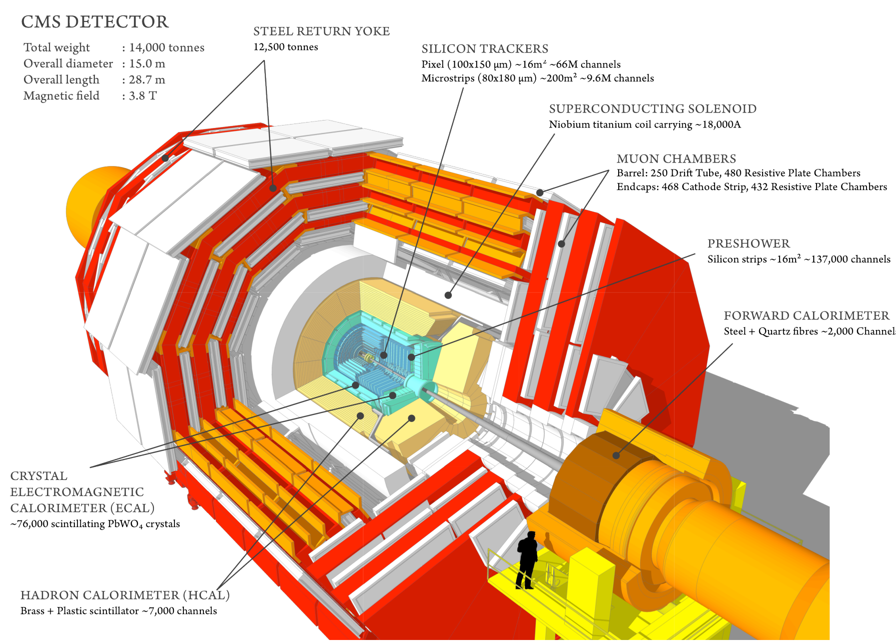

CMS

Different jet flavours result in different analyses!

$t\bar{t}$ + jets

ATLAS Collaboration, *$t\bar{t}$ +jets differential cross sections (ℓ +jet)*, Eur. Phys. J. C 79 (2019) 12, 1028

ATLAS Collaboration, *jet activity in $t\bar{t}$ production ($e\mu$)*, Eur. Phys. J. C 77 (2017) 4, 220

ATLAS Collaboration, *$t\bar{t}$ differential cross sections (all hadronic)*, Arxiv: 2006.09274 (Sub. To JHEP)

ATLAS Collaboration, *$t\bar{t}$ +jets differential cross sections (ℓ +jet)*, JHEP 10 (2018), 159

CMS Collaboration, *$t\bar{t}$ +jets differential cross sections (ℓ +jet)*, Phys.Rev.D 97 (2018) 11, 112003

CMS Collaboration, *$t\bar{t}$ differential cross sections (dilepton)*, Eur. Phys. J. C 80 (2020) 7, 658

Different jet flavours result in different analyses!

$t\bar{t}$ + jets

ATLAS Collaboration, *$t\bar{t}$+jets differential cross sections (ℓ+jet)*, Eur. Phys. J. C 79 (2019) 12, 1028

ATLAS Collaboration, *jet activity in $t\bar{t}$ production (eμ)*, Eur. Phys. J. C 77 (2017) 4, 220

ATLAS Collaboration, *$t\bar{t}$ differential cross sections (all hadronic)*, Arxiv: 2006.09274 (Sub. To JHEP)

ATLAS Collaboration, *$t\bar{t}$+jets differential cross sections (ℓ+jet)*, JHEP 10 (2018), 159

CMS Collaboration, *$t\bar{t}$+jets differential cross sections (ℓ+jet)*, Phys.Rev.D 97 (2018) 11, 112003

CMS Collaboration, *$t\bar{t}$ differential cross sections (dilepton)*, Eur. Phys. J. C 80 (2020) 7, 658

$t\bar{t}$ + heavy-flavour (HF) jets

ATLAS Collaboration, $t\bar{t}b(\bar{b})$ *(inclusive/differential + dilepton/ℓ+jet)*, JHEP 04 (2019), 046

CMS Collaboration, $t\bar{t}b\bar{b}$ *inclusive (dilepton/ℓ+jet)*, JHEP 07 (2020), 125

CMS Collaboration, $t\bar{t}b\bar{b}$ *inclusive (all hadronic)*, Phys.Lett.B 803 (2020), 135285

CMS Collaboration, $t\bar{t}c\bar{c}$ *inclusive (dilepton)*, Physics Analysis Summary TOP-20-003

Overview

Different jet flavours result in different analyses!

$t\bar{t}$ + jets

ATLAS Collaboration, *$t\bar{t}$+jets differential cross sections (ℓ+jet)*, Eur. Phys. J. C 79 (2019) 12, 1028
ATLAS Collaboration, *jet activity in $t\bar{t}$ production (eμ)*, Eur. Phys. J. C 77 (2017) 4, 220
ATLAS Collaboration, *$t\bar{t}$ differential cross sections (all hadronic)*, Arxiv: 2006.09274 (Sub. To JHEP)
ATLAS Collaboration, *$t\bar{t}$+jets differential cross sections (ℓ+jet)*, JHEP 10 (2018), 159

CMS Collaboration, *$t\bar{t}$+jets differential cross sections (ℓ+jet)*, Phys.Rev.D 97 (2018) 11, 112003
CMS Collaboration, *$t\bar{t}$ differential cross sections (dilepton)*, Eur. Phys. J. C 80 (2020) 7, 658

$t\bar{t}$ + heavy-flavour (HF) jets

ATLAS Collaboration, *$t\bar{t}b(\bar{b})$ (inclusive/differential + dilepton/ℓ+jet)*, JHEP 04 (2019), 046

CMS Collaboration, *$t\bar{t}b\bar{b}$ inclusive (dilepton/ℓ+jet)*, JHEP 07 (2020), 125

CMS Collaboration, *$t\bar{t}b\bar{b}$ inclusive (all hadronic)*, Phys.Lett.B 803 (2020), 135285

CMS Collaboration, *$t\bar{t}c\bar{c}$ inclusive (dilepton)*, Physics Analysis Summary TOP-20-003

Older references

ATLAS Collaboration, *$t\bar{t}$+HF inclusive (dilepton, 7 TeV, 4.7 fb^{-1})*, Phys.Rev.D 89 (2014) 7, 072012
ATLAS Collaboration, *$t\bar{t}b\bar{b}$ inclusive (dilepton/ℓ+jet 8TeV, 20.3 fb^{-1})*, Eur.Phys.J.C 76 (2016) 1, 11

CMS Collaboration, *$t\bar{t}b\bar{b}$ inclusive (dilepton 13TeV, 2.3 fb^{-1})*, Phys.Lett.B 776 (2018), 355-378
CMS Collaboration, *$t\bar{t}b\bar{b}$ inclusive (dilepton 8TeV, 19.6 fb^{-1})*, Phys.Lett.B 746 (2015), 132-153
CMS Collaboration, *$t\bar{t}b\bar{b}$ differential (dilepton 8TeV, 19.6 fb^{-1})*, Eur.Phys.J.C 76 (2016) 7, 379

$t\bar{t}$ + jets

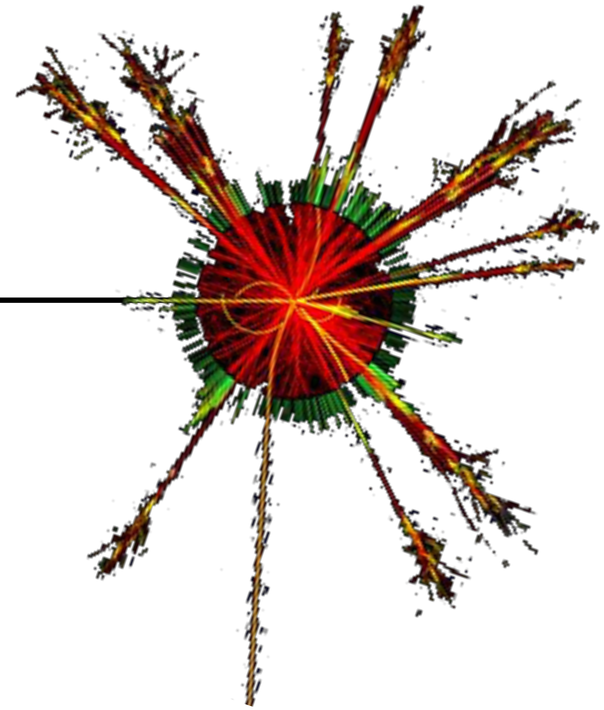

$t\bar{t}$ + jets
A selection of ATLAS highlights (36.1/3.2 fb^{-1})

Eur. Phys. J. C 79 (2019) 12, 1028

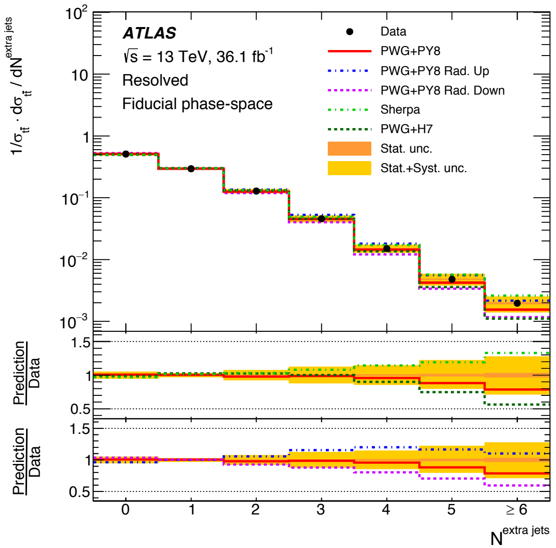

Differential $t\bar{t}$ cross section measurement **as a function of kinematics of the $t\bar{t}$ system and jet multiplicities** are presented (in resolved and boosted topologies)

These provide important constraints to several generator setups! **(Many results of which I highlight only one!)**

Figure shows the normalized differential cross section as a function of the number of additional jets (p_T > 25 GeV), with good agreement up to 3 additional jets, and some tension at higher jet multiplicities.
→ **p-values ranging from <0.01 to 0.44** [link]

Differential $t\bar{t}$ cross section measurement **as a function of** (top decay and) **additional jet kinematics** are presented.

Gap fraction = fraction of events without any additional radiation above a given kinematic threshold (p_T or H_T).

This is an interesting quantity that provides complementary information on additional jet kinematics rather than additional jet multiplicity.

Significant differences are observed between generators and between data and simulation. → **p-values ranging from 3.4×10^{-6} to 0.89** [link]
some MC settings have been tuned after this early 13 TeV measurement

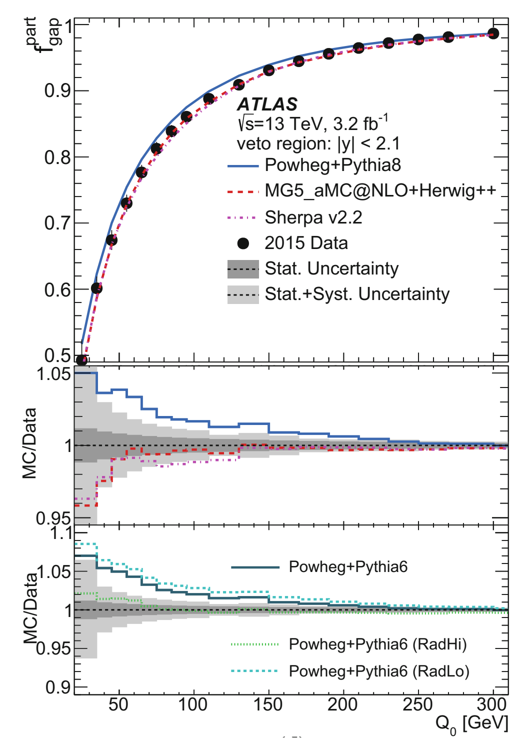

Eur. Phys. J. C 77 (2017) 4, 220

$t\bar{t}$ + jets

A selection of CMS highlights (35.8 fb^{-1})

CMS result with **35.8 fb^{-1}** (2016) → [Phys.Rev.D 97 (2018) 11, 112003]

Amongst a very rich content of differential measurements, results on **$t\bar{t}$ cross section as a function of additional jet multiplicity for different p_T thresholds** are shown below.

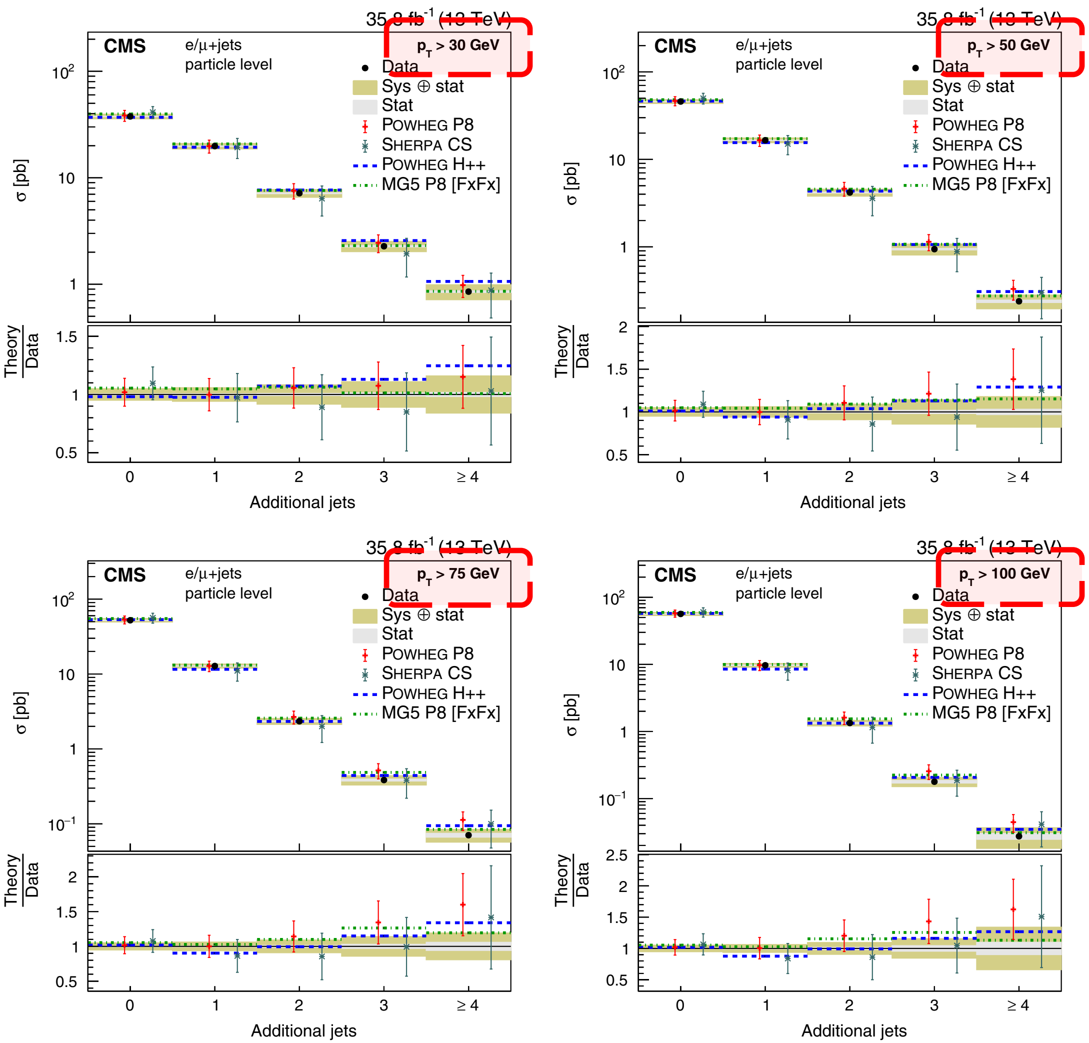

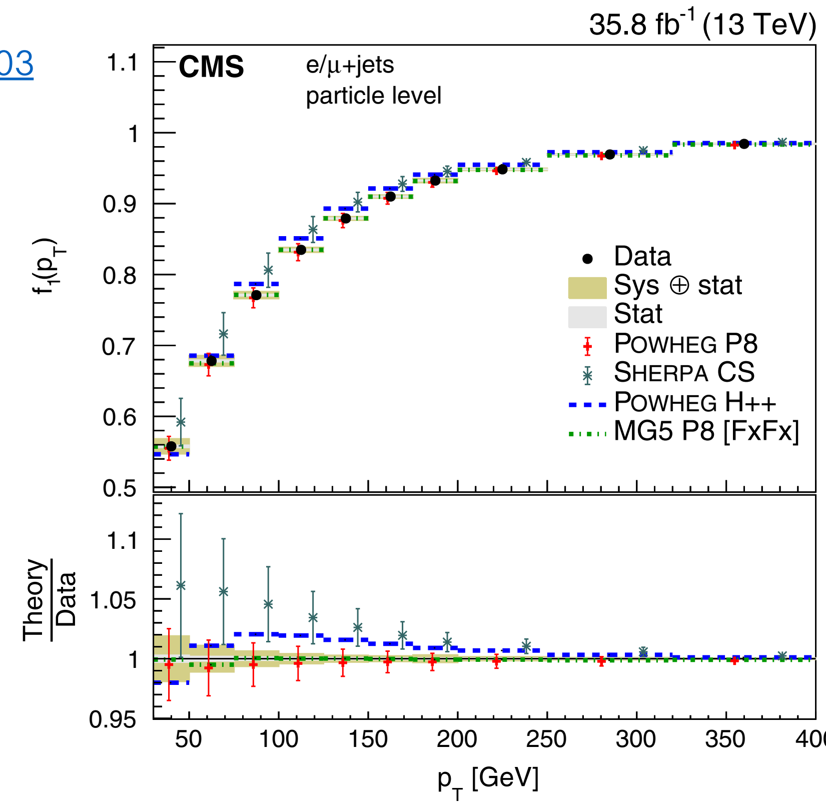

The **gap fraction** is also measured by CMS.

Increased sensitivity results in **uncertainties at the O(1%)** level (more accurate than the predictions from simulations)!

→ data provides constraints on theory.

Description from Powheg+Pythia8 seems to follow the data much better compared to the ATLAS configuration with the same ME/PS.

$t\bar{t}$ + heavy-flavour jets

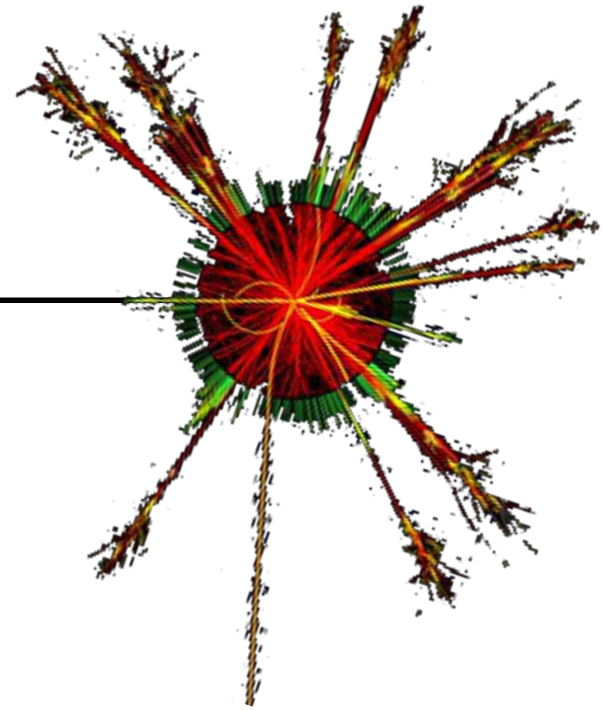

Theoretical modelling of $t\bar{t}$+HF

Simulating these processes remains an active field of study

Theory predictions / Simulation of the $t\bar{t}$+HF final state is highly non-trivial. It deals with very different scales from the top quark mass down to momenta of the relatively soft additional jets.

- Matrix Element vs Parton Shower.
- $t\bar{t}b\bar{b}$@LO vs NLO vs $t\bar{t}b\bar{b}j$@NLO (large k-factor, depending on scale choice) [Buccioni F. et al, JHEP 12 (2019), 015].
- Factorization/Renormalization/Shower/matching scales.
- Inclusive $t\bar{t}$+jets versus dedicated $t\bar{t}b\bar{b}$ and $t\bar{t}c\bar{c}$ simulation.

Still a very active field of study!
[Sigert F, Jan 2020, Zürich Phenomenology Workshop]
[Pozorrini et al., October 2020, ttH-HXSWG meeting]

→ Important backgrounds to $t\bar{t}H$ ($H \rightarrow b\bar{b}$) measurements!

T.0Ježo et al., *Eur. Phys. J.* **C78** (2018), no. 6 502, [arXiv:1802.00426]

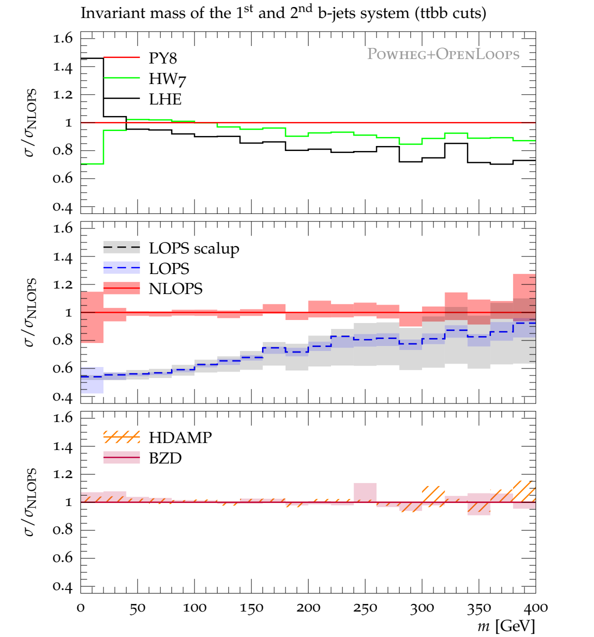

ATL-PHYS-PUB-2016-011

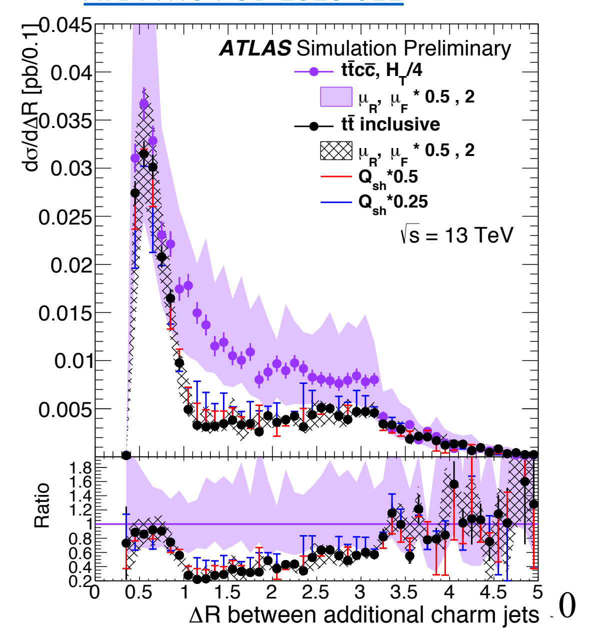

S. Pozzorini, Theory progress on $t\bar{t}H(b\bar{b})$ background, TOP2018 @ Bad Neuenahr, Germany

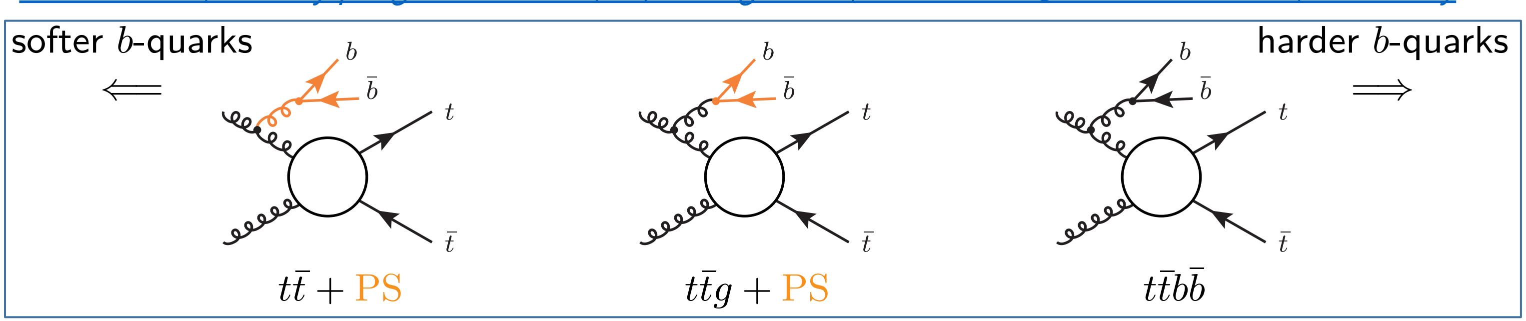

A very **detailed** **exploration** of the $t\bar{t}b\bar{b}$ landscape

Dilepton / ℓ+jet

Inclusive / differential cross sections

JHEP 04 (2019), 046

ME comparisons:
Powheg, MadGraph, Sherpa, PowHel
inclusive / $t\bar{t}b\bar{b}$ in the ME

PS comparisons:
Pythia, Herwig, Sherpa

The ATLAS $t\bar{t}b(\bar{b})$ measurement

Fitting normalization of different flavour components

Differential $t\bar{t}$+jet measurements are agnostic about jet flavour.

→ The normalizations of $t\bar{t}$+>1b, $t\bar{t}$+>1c, and $t\bar{t}$+>1l are fitted in a "control region"

1. Rank jets according to the b-tagging discriminator value
2. Take the 3rd (and 4th in ℓ+jet) ranked jet (proxies for additional radiation)
3. Divide in bins that represent different b-tagging efficiency ranges(*)

eμ channel, ≥ 3b

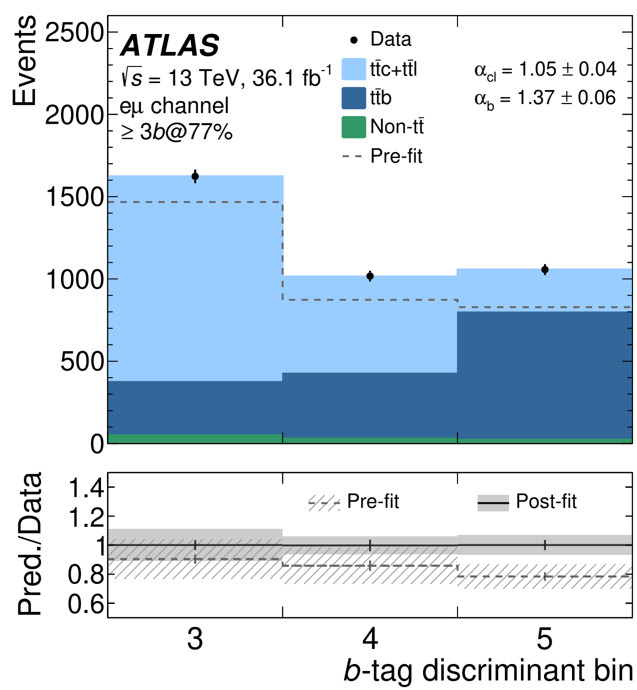

ℓ+jet channel, ≥ 5j, ≥ 2b

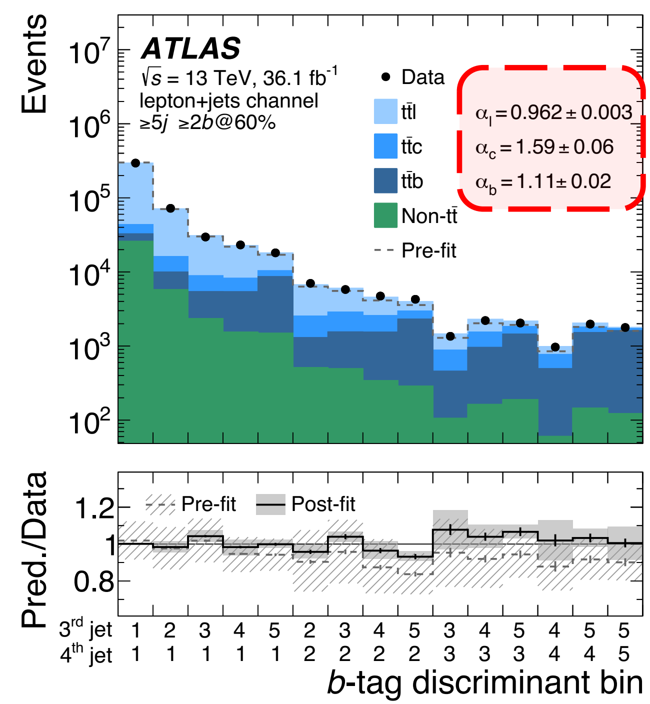

*stat. unc. only

(*)

Bin	Efficiency
1	100%-85%
2	85%-77%
3	77%-70%
4	70%-60%
5	<60%

The ATLAS $t\bar{t}b(\bar{b})$ measurement

Results of the inclusive measurement

Inclusive fiducial cross sections are reported (backgrounds and ttH/ttV "signals" are subtracted using MC predictions)

Separate results for ≥ 3b and ≥ 4b (i.e. for ≥1 or ≥2 'additional' b jets)

Uncertainties dominated by systematics: b-tagging, Jet Energy Scale, Modelling (PS)

Compared to several simulations
→ **Overall higher $t\bar{t}b(\bar{b})$ cross section observed in data** compared to MC predictions!

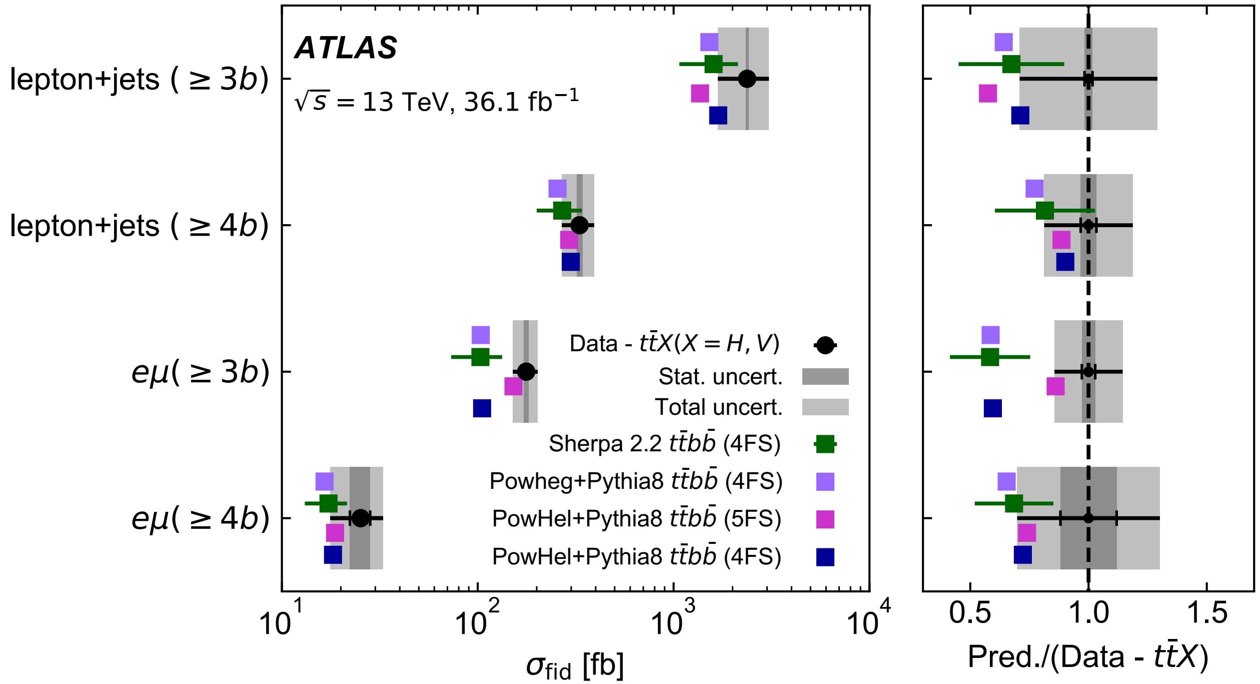

The ATLAS $t\bar{t}b(\bar{b})$ measurement

Differential measurements to explore the entire topology

p_T of the 3[rd] hardest b jet
→ probe **additional b jet kinematics**

ΔR between the two closest b jets
→ probe **angular correlations between additional b jets** (colinear gluon splitting into $b\bar{b}$)

Invariant mass between the two leading (hardest) b jets
→ probe the kinematic **properties of the $t\bar{t}$ system**

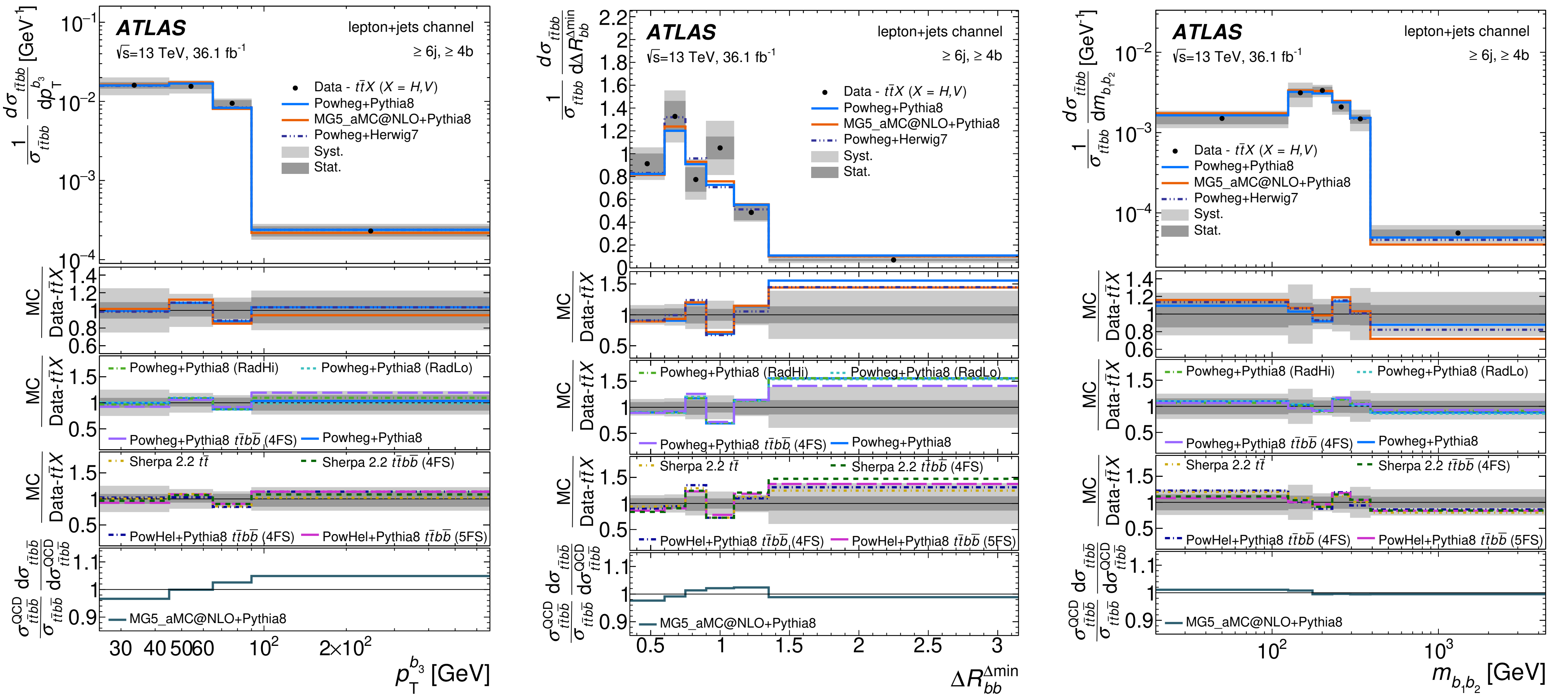

→ p-values ranging from 0.49 to 0.73

→ p-values ranging from 0.48 to 0.70

→ p-values ranging from 0.53 to 0.89

Overall good agreement between data and simulation!

The ATLAS $t\bar{t}b(\bar{b})$ measurement

An interesting part of the conclusion

edge of the phase space for some of the observables. The observables are well described by most MC predictions in both channels. However, it is worth noting that in all the predictions where additional *b*-jets are dominantly produced by the parton shower, they predict too few events with more *b*-jets than those produced in top decays. Only SHERPA 2.2 $t\bar{t}$ describes the full *b*-jet multiplicity spectrum, and in events with ≥ 3 *b*-jets it yields the best agreement with data in most of the observables. POWHEL+PYTHIA 8 $t\bar{t}b\bar{b}$ (5FS) shows poor agreement in some of the observables in events with ≥ 3 *b*-jets in the $e\mu$ channel. The differential kinematic distributions are equally well described by predictions that

"Additional b jets produced by the PS = underestimation (25-50%) in high b jet multiplicity"

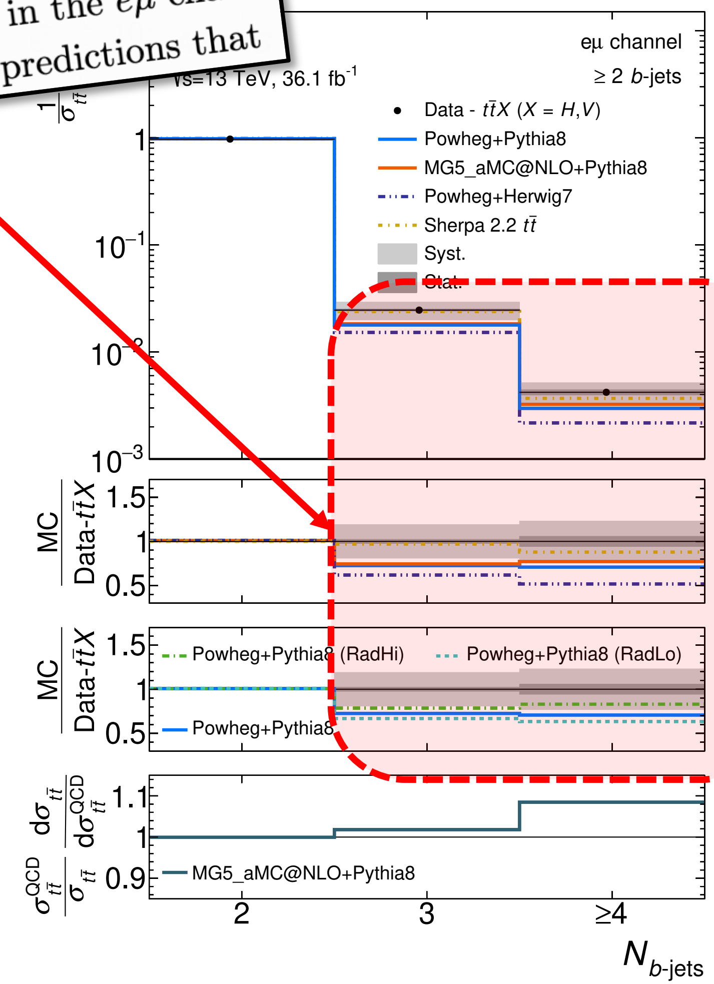

The CMS dilepton/ ℓ+jet $t\bar{t}b\bar{b}$ measurement

The strategy outlined

JHEP 07 (2020), 125

	Dilepton	ℓ+jet
Baseline selection	$2\ell, \geq 4j, \geq 2$b-tag	$1\ell, \geq 6j, \geq 2$b-tag
Identify additional jets	3rd and 4th largest b-tagging discriminator score	Kinematic fit to reconstruct $t\bar{t}$ system + take largest remaining b-tag scores
Extract results	2D template fit → extract $\sigma_{t\bar{t}jj}$ and $R_{t\bar{t}b\bar{b}/t\bar{t}jj} = {}^{\sigma_{t\bar{t}b\bar{b}}}/_{\sigma_{t\bar{t}jj}}$	

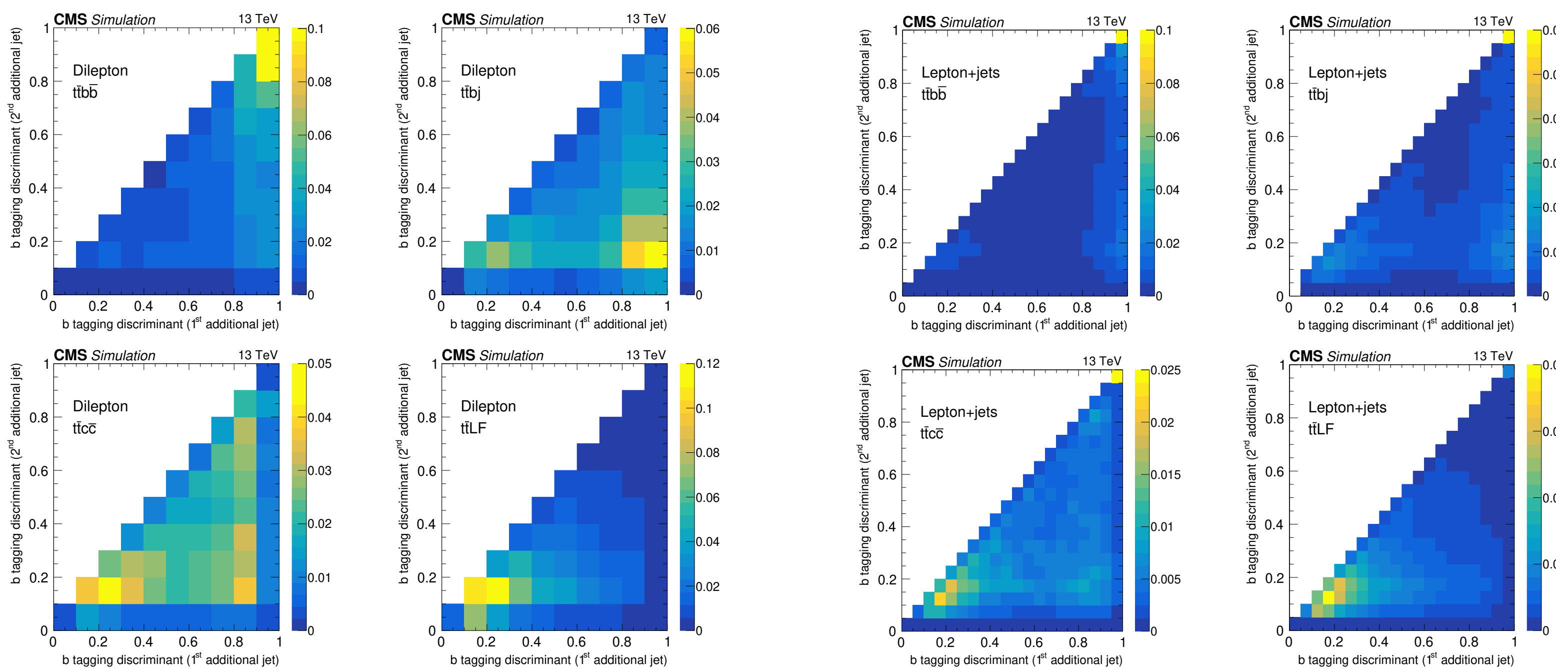

The CMS dilepton/ ℓ+jet $t\bar{t}b\bar{b}$ measurement
Results

Inclusive cross sections (and ratio) measured in the fiducial phase space and unfolded into the full phase space → Acceptance and efficiency corrections derived from simulations.

Uncertainties dominated by b-tagging and theoretical modeling (ME/PS scales)

Precision of ~ 13% on $\sigma_{t\bar{t}b\bar{b}}$

$\sigma_{t\bar{t}jj}$ well modelled, but $R_{t\bar{t}b\bar{b}/t\bar{t}jj}$ (and therefore also $\sigma_{t\bar{t}b\bar{b}}$) underestimated in the simulation.

Dilepton ℓ+jet

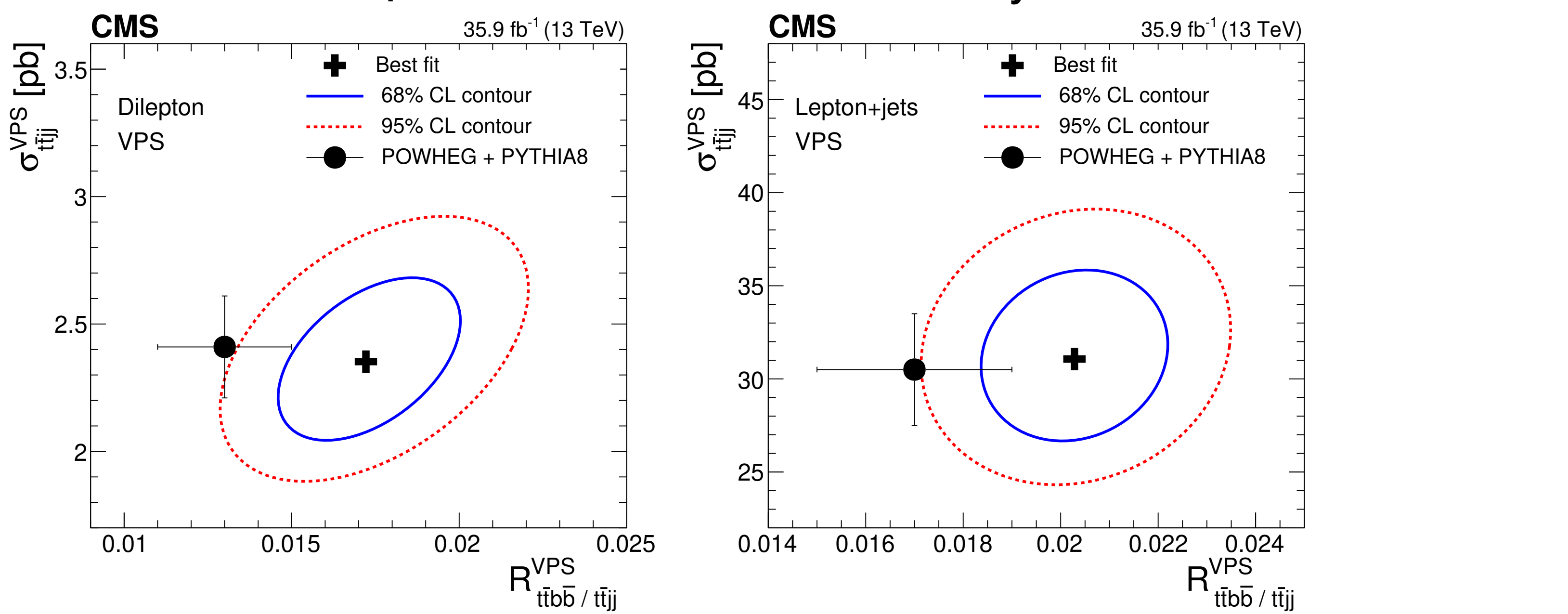

The CMS fully hadronic $t\bar{t}b\bar{b}$ measurement

The strategy outlined

Phys.Lett.B 803 (2020), 135285

Baseline selection

$0\ell, \geq 8j, \geq 2b$-tag

Identify additional jets

BDT trained to identify jets from $t\bar{t}$ decays

Reduce QCD background

Quark-gluon likelihood ratio

"QCD events expected to have more gluon jets"

CWoLa BDT JHEP 10 (2017), 174

Unsupervised learning on data in control regions (==7 jets) with mixed signal/bkg compositions

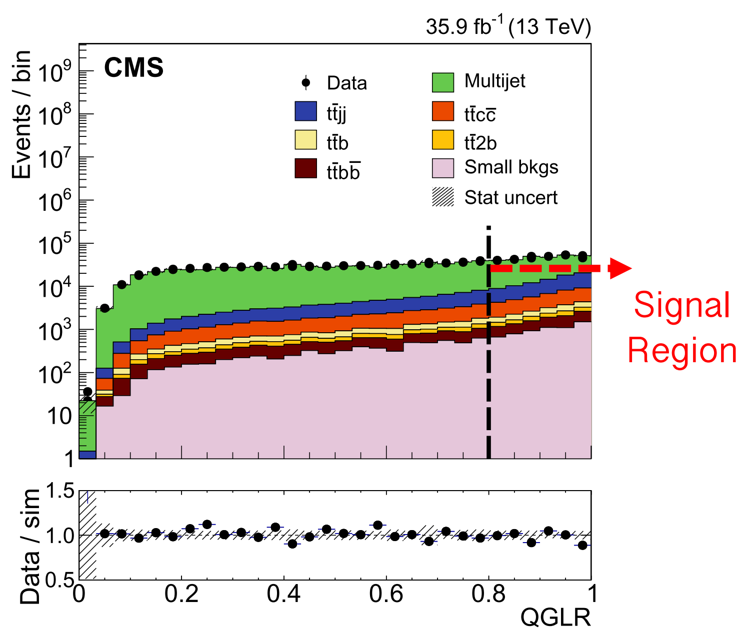

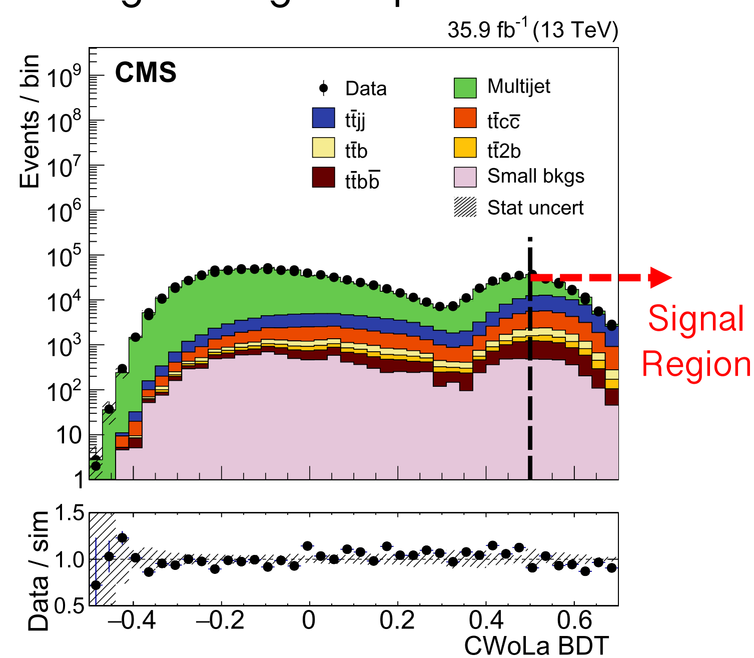

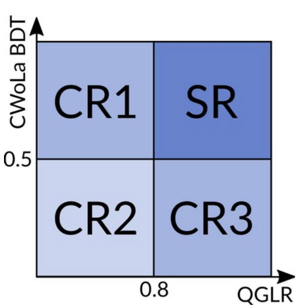

Uncorrelated observables → ABCD method to estimate QCD contributions in the final fit

The CMS fully hadronic $t\bar{t}b\bar{b}$ measurement
2D template fit to extract the results

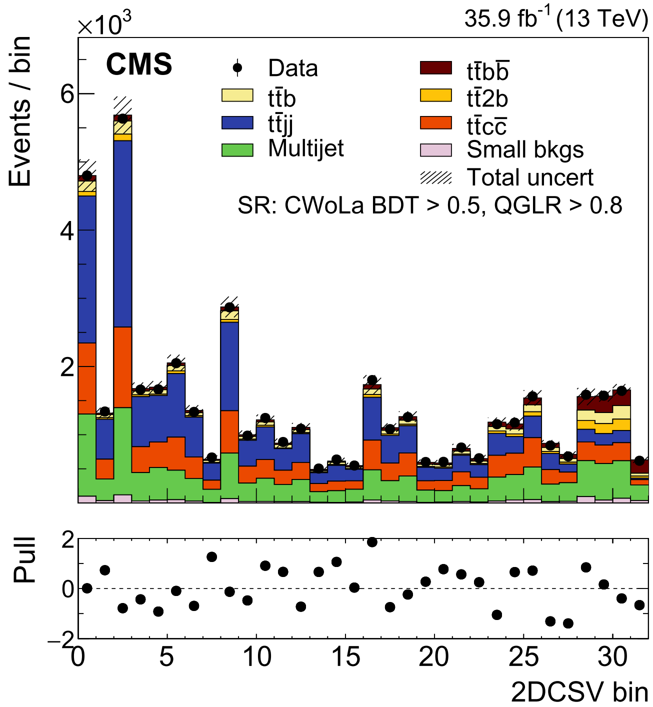

Fit in (2D) bins of b-tagging score of the two additional jets

Uncertainties dominated by QGLR and b-tagging calibrations + signal/background modelling.

Precision of ~ 30%!

Again, $\sigma_{t\bar{t}b\bar{b}}$ is under-predicted in the simulation.

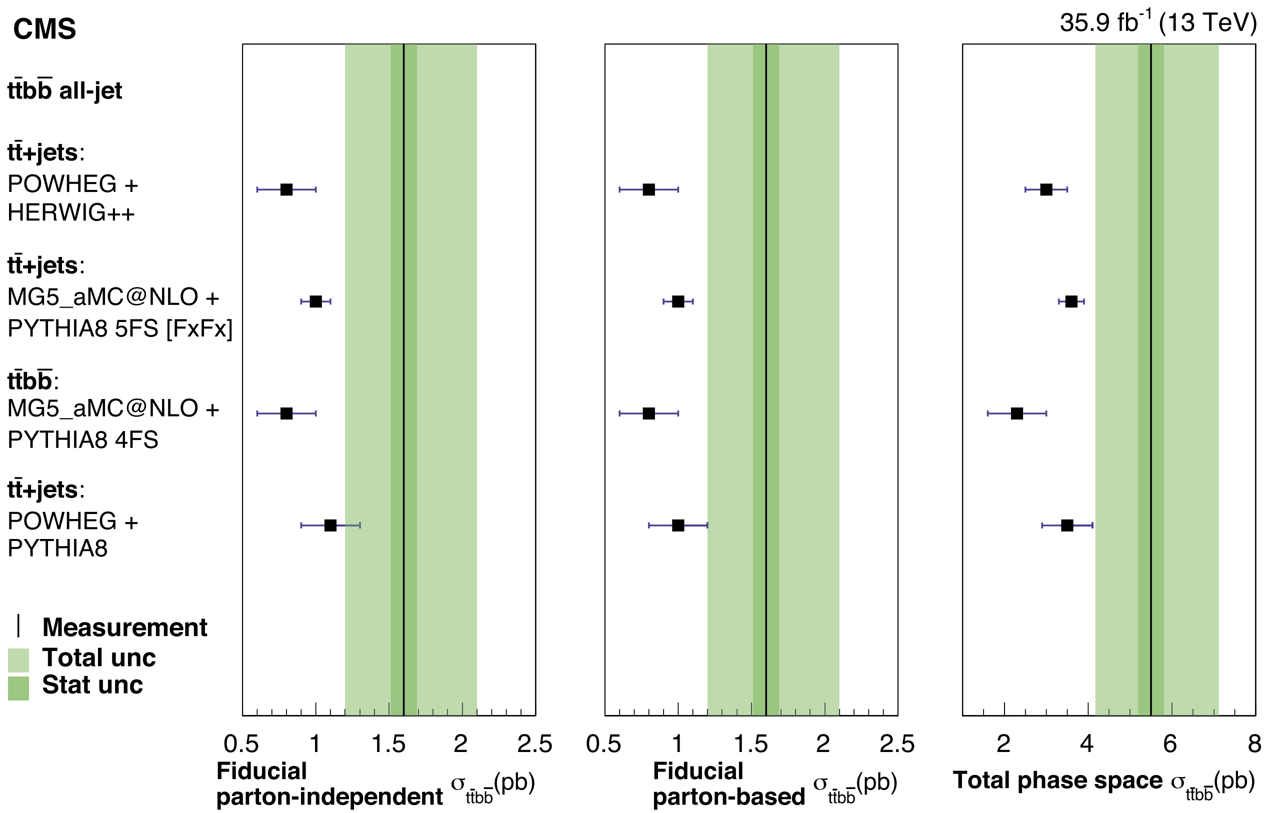

Comparison of the CMS $t\bar{t}b\bar{b}$ measurements

Consistently, the $t\bar{t}b\bar{b}$ cross section is under-estimated in simulations

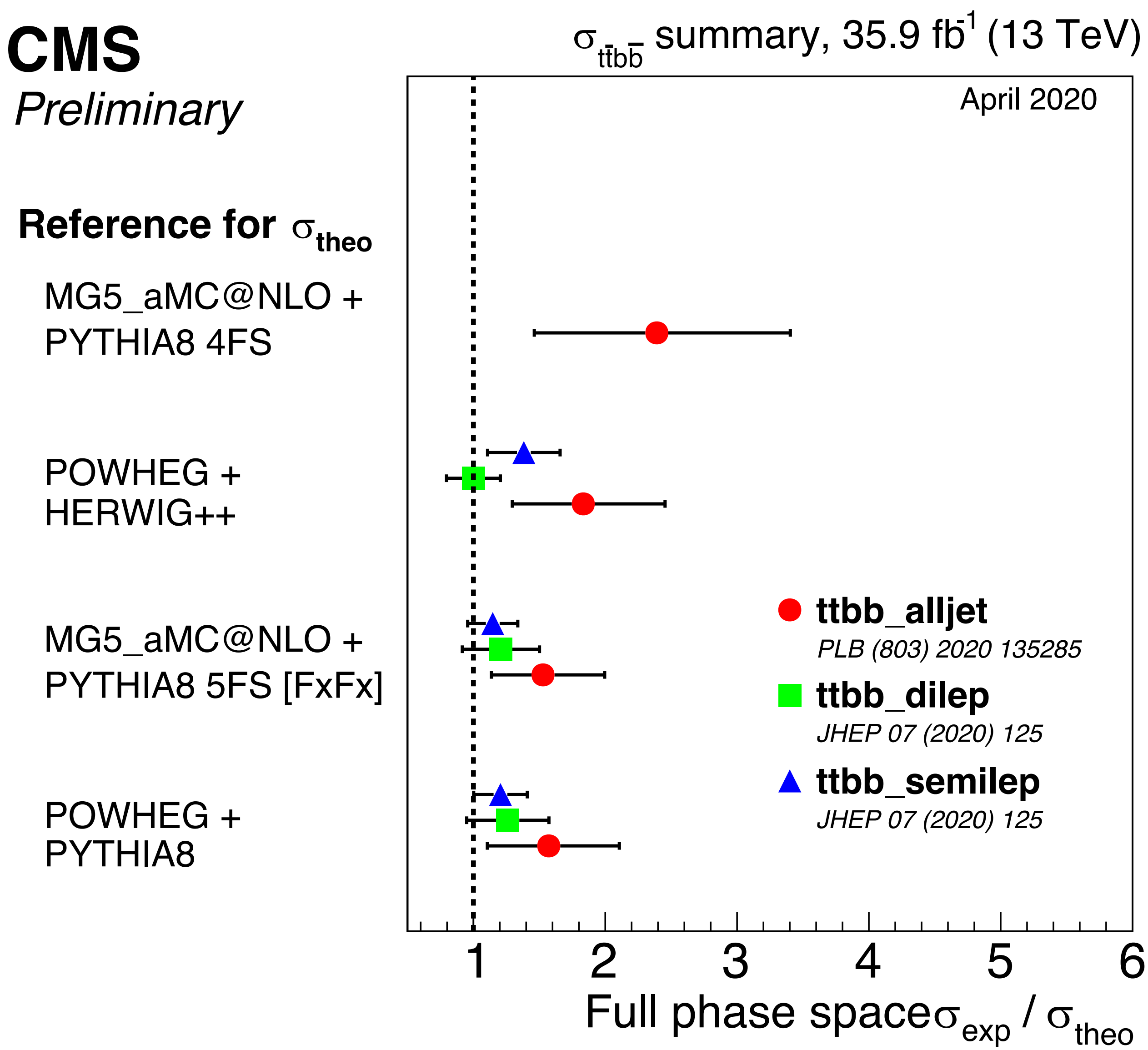

$t\bar{t}$ + charm jets! (NEW)

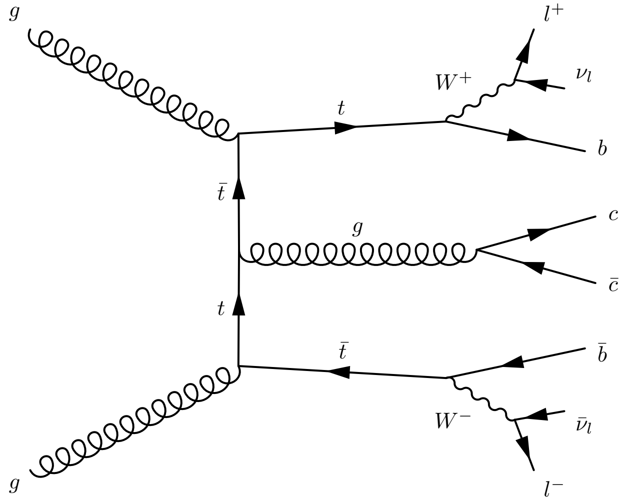

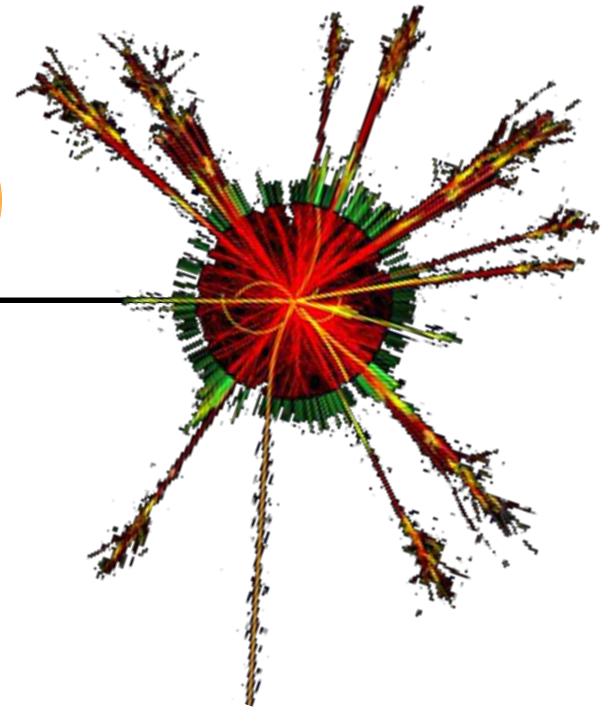

Physics Analysis Summary TOP-20-003

Goal and scope

First measurement of the $t\bar{t} + c\bar{c}$ cross section, but simultaneously measure $\sigma(t\bar{t}+b\bar{b})$, $\sigma(t\bar{t}+\mathrm{LF})$ and $R_{c/b} = \sigma(t\bar{t}+c\bar{c}/b\bar{b}) / \sigma(t\bar{t}+jj)$

Measurement performed in the dilepton channel, using 2017 dataset, 41.5 fb^{-1}

Baseline selection

$2\ell, \geq 4j, \geq 2b\text{-tag}$

Identify additional jets

NN trained to identify additional HF jets

Use charm jet identification (c-tagging)

Properties from c jets are distributed midway between those of b or light-flavour jets → two c-tagging discriminants!

$$P(\mathrm{CvsL}) = \frac{P(c)}{P(c) + P(udsg)}, \qquad P(\mathrm{CvsB}) = \frac{P(c)}{P(c) + P(b) + P(bb)}.$$

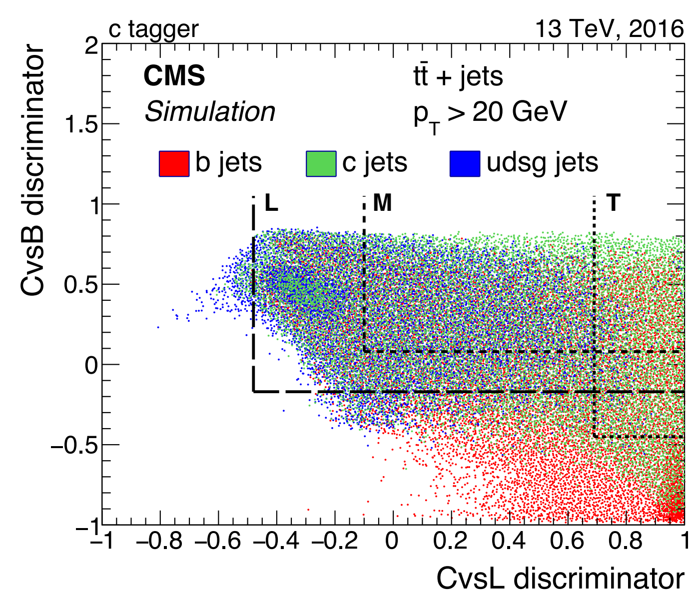

The CMS dilepton $t\bar{t}c\bar{c}$ measurement

Calibration of the c-tagger shape

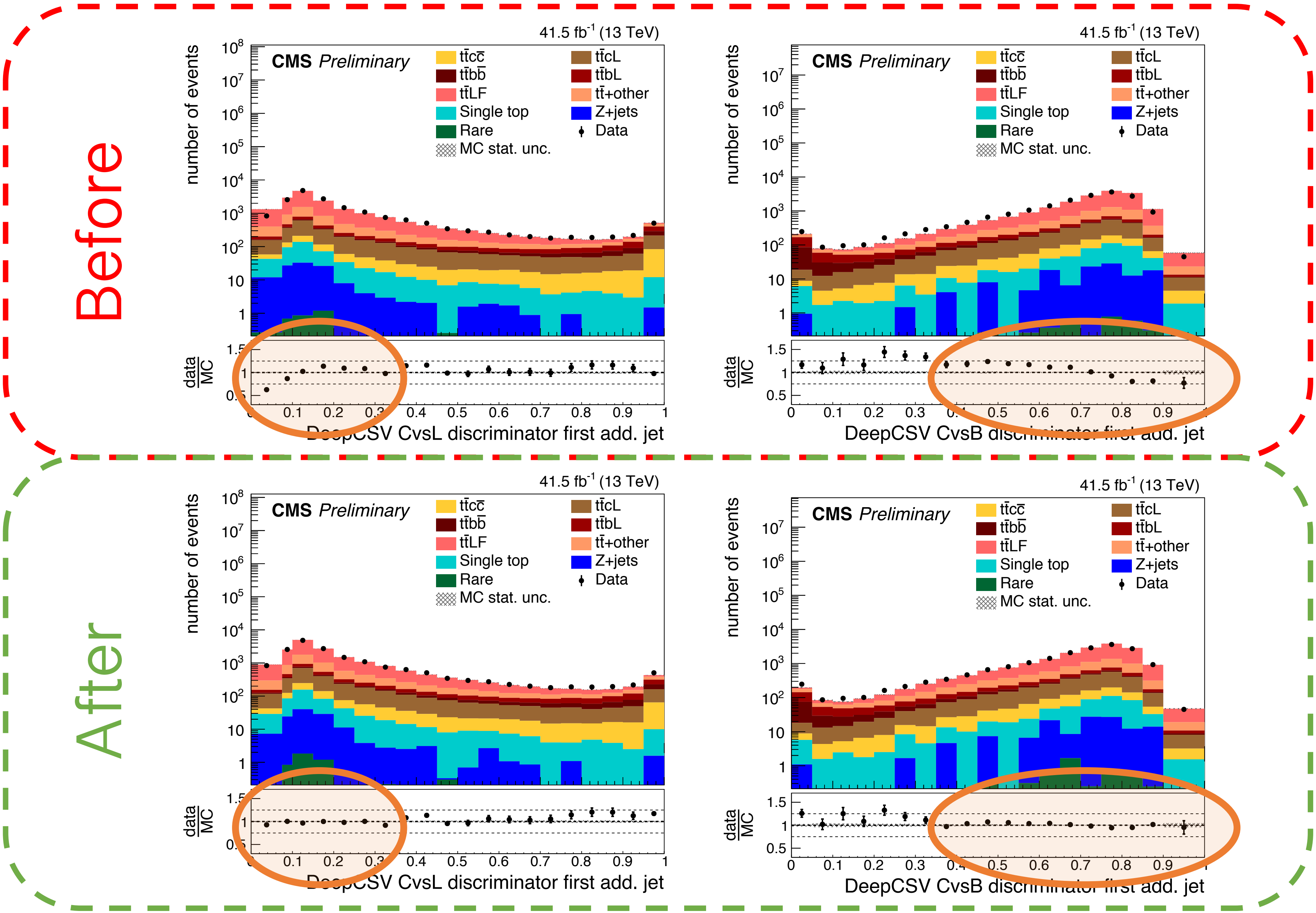

The CMS dilepton $t\bar{t}c\bar{c}$ measurement
Two-dimensional simulated templates used in the fit

Another NN is trained to distinguish $t\bar{t}c\bar{c}$ from $t\bar{t}b\bar{b}$ (Δ_b^c) and from $t\bar{t}$LF (Δ_L^c).

The fit is performed on two-dimensional distributions. Uncertainties dominated by c-tagging calibration, JES, modelling (ME and PS scales and matching)

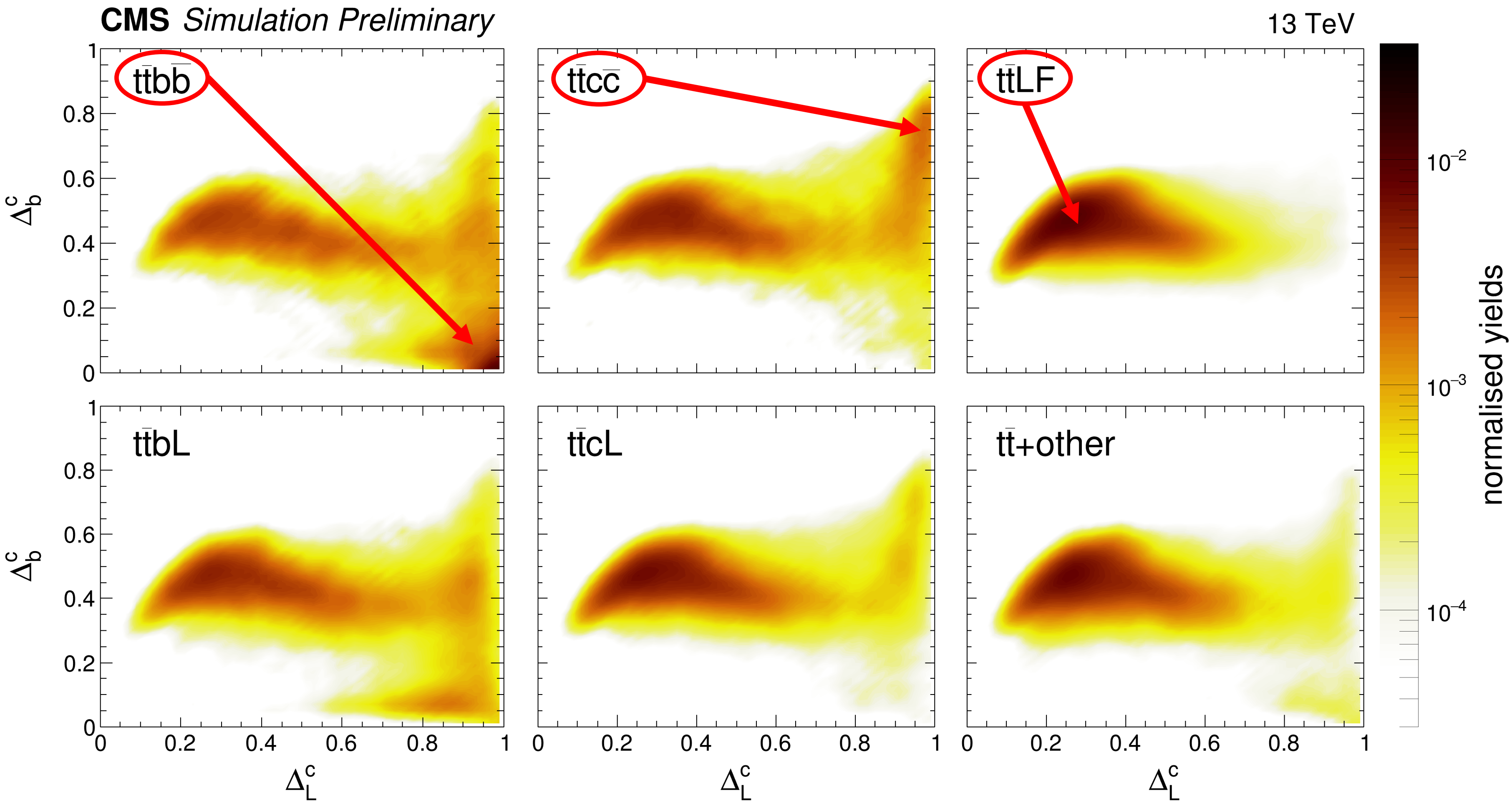

Clear separation between the $t\bar{t}b\bar{b}$, $t\bar{t}c\bar{c}$ and $t\bar{t}$LF contributions

The CMS dilepton $t\bar{t}c\bar{c}$ measurement

Summary of the results

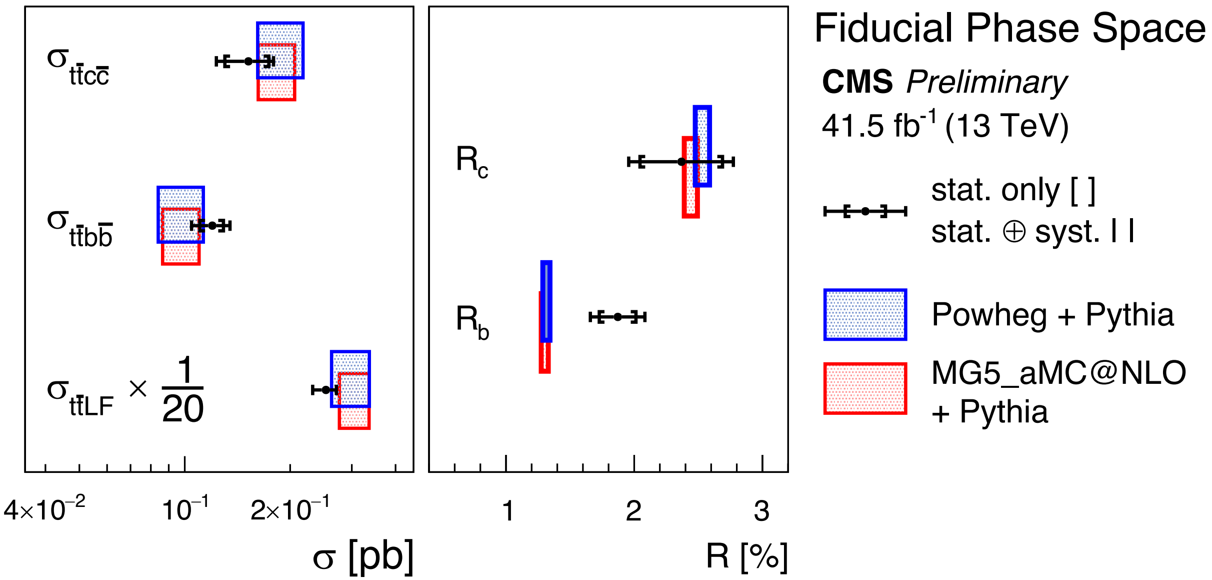

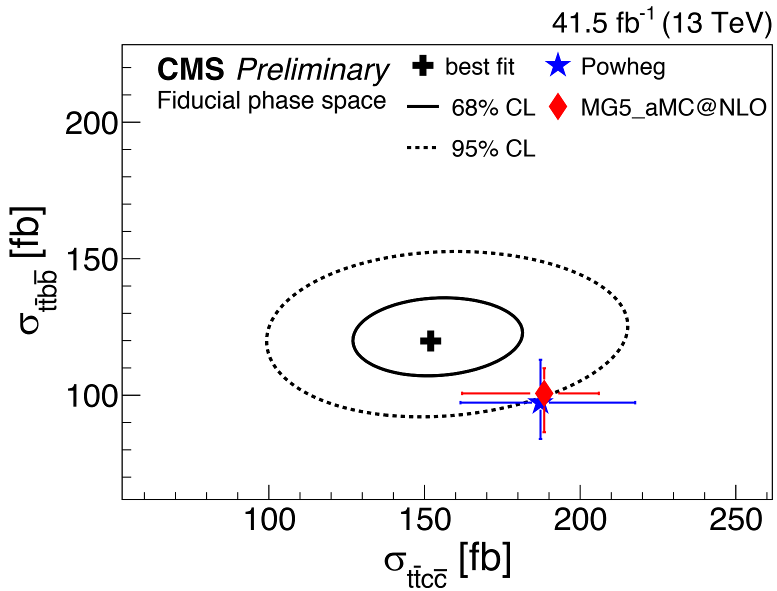

First measurement of the $t\bar{t} + c\bar{c}$ cross section!

Fiducial PS:

$\sigma(t\bar{t} + c\bar{c})$ = 152 ± 22 (stat.) ± 19 (syst.) fb (~ 19% uncertainty)

Rc = 2.37 ± 0.32 (stat.) ± 0.25 (syst.) % (~ 17% uncertainty)

Full PS:

$\sigma(t\bar{t} + c\bar{c})$ = 7.43 ± 1.07 (stat.) ± 0.95 (syst.) pb

Rc = 2.64 ± 0.36 (stat.) ± 0.29 (syst.) %

Also in this analysis we see an **underestimation of $\sigma(t\bar{t}+b\bar{b})$ and R_b, but an overestimation of $\sigma(t\bar{t}+c\bar{c})$ and $\sigma(t\bar{t}+LF)$** (everything within 1-2 stdandard deviations)

ATLAS $t\bar{t}c$ reco-level scaling factor (slide 12): $\alpha_c^{ATLAS} = 1.59 \pm 0.06$ (stat) ± 0.7 (model) hints at **underestimation of ttc signal strength** in MC, whereas CMS observes: $\alpha_c^{CMS} = 0.81 \pm 0.12$ (stat) ± 0.10 (syst)

Conclusions

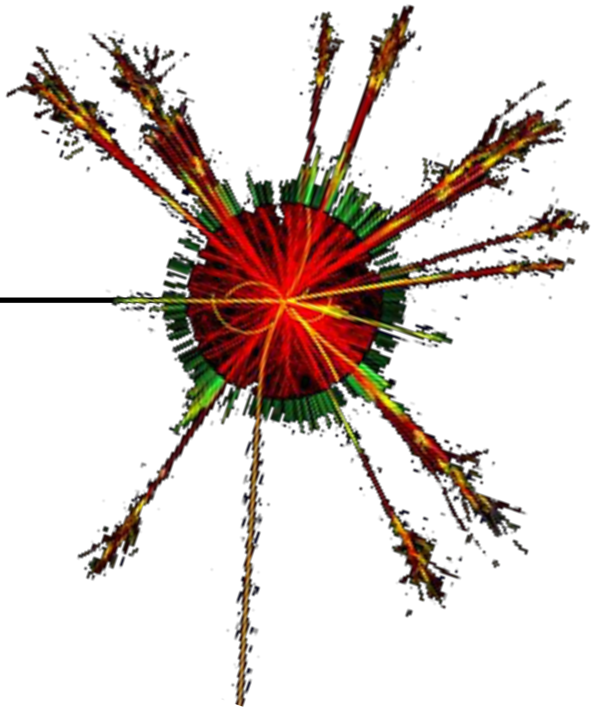

Summary and conclusions

Differential $t\bar{t}$+jets analyses from CMS and ATLAS allow to probe kinematics of the additional radiation (PS) and puts different ME/PS simulators to the test.
→ Full Run-2 combinations of these analyses will greatly improve the precision (lower statistical errors allow for much finer binning!)

Both CMS and ATLAS have explored the **$t\bar{t}b\bar{b}$ landscape** in different channels using the 2016 dataset, reaching a **precision of roughly 13-16%.**
→ Consistent **underestimation of $\sigma(t\bar{t}b\bar{b})$** in different simulators.
→ CMS managed to conquer the fully-hadronic channel.
→ ATLAS provided a first set of differential measurements.

CMS presented a **first measurement of $\sigma(t\bar{t}c\bar{c})$** with a precision of around 20%.
→ CMS result reveals a slight overestimation of $t\bar{t}c\bar{c}$ yield in MC (within unc.)
→ charm-tagging tools (and calibration) are a vital component.
→ ATLAS scaling factor for $t\bar{t}c$ at detector level hints at possibly underestimation ttc signal strength in MC compared to data

<u>**Important steps in my opinion:**</u>
→ Come up with a **uniform phase space definition** for fair comparisons.
→ Stay in touch with the **theory community** to improve the simulations.
→ Work towards **full Run-2** results (all channels, inclusive+differential, $t\bar{t}c\bar{c}$, $t\bar{t}b\bar{b}$, $t\bar{t}$LF)
→ **EFT** interpretation? (qqqq and qqH operators in a combined tt+HF/tttt/ttH interp.)

Backup

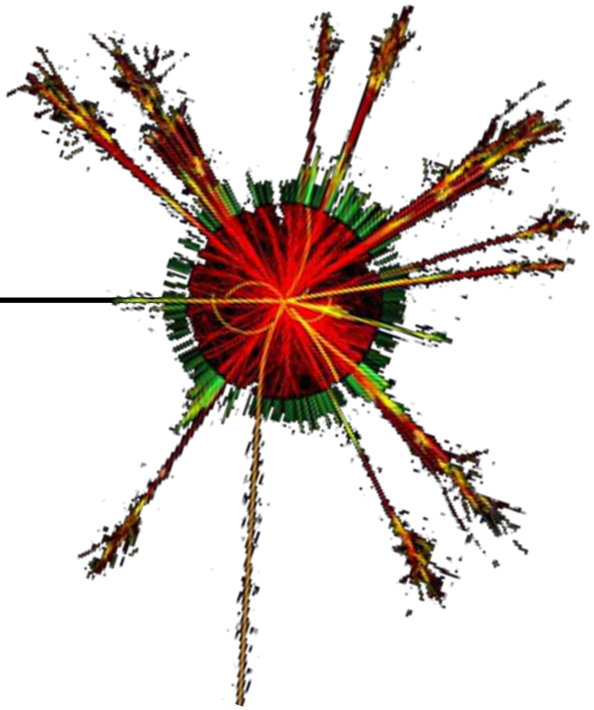

Some additional ATLAS differential measurements

ATLAS Collaboration, *$t\bar{t}$+jets differential cross sections (ℓ+jet)*, JHEP 10 (2018), 159

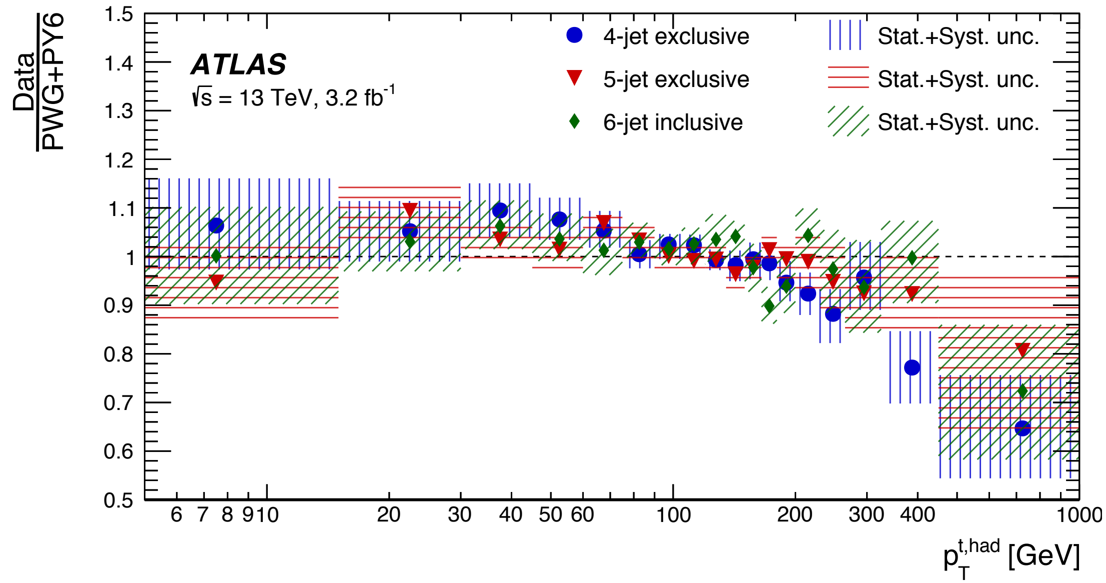

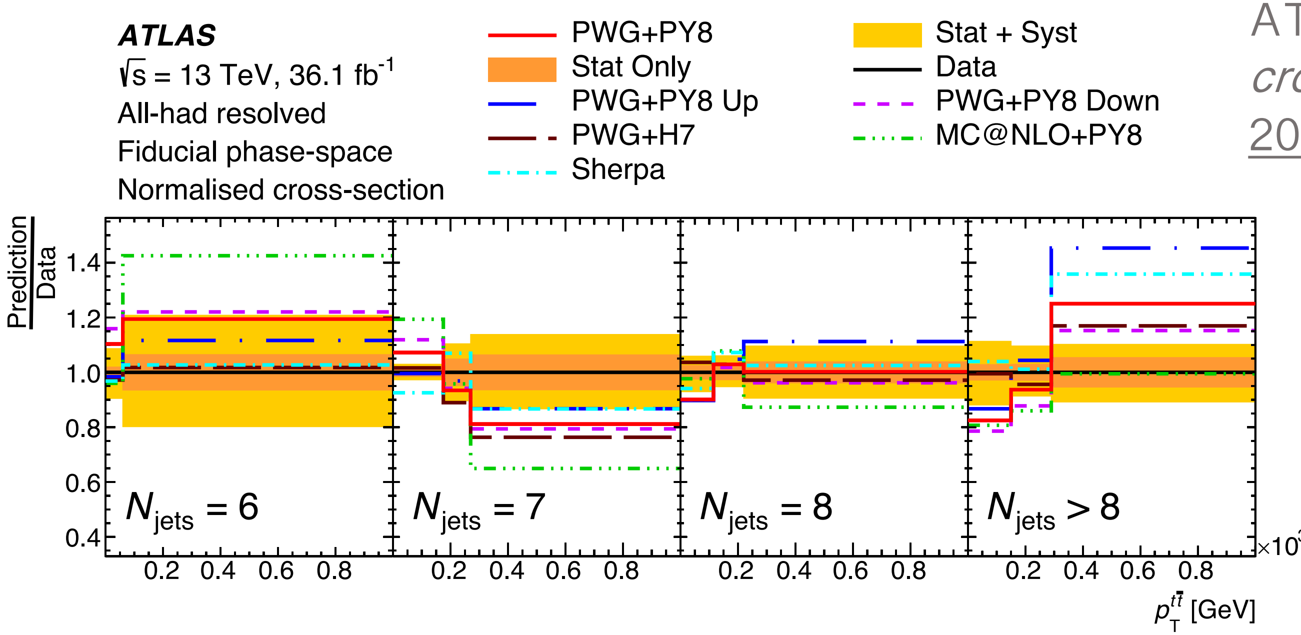

ATLAS Collaboration, *$t\bar{t}$ differential cross sections (all hadronic)*, Arxiv: 2006.09274 (Sub. To JHEP)

The ATLAS $t\bar{t}b(\bar{b})$ measurement

Uncertainties in the differential measurement

Normalized differential cross sections as a function of a large variety of kinematical quantities are unfolded to particle-level.

Differential measurements suffer more from statistical limitations (especially the eμ channel which is only probed differentially in the $\geq 3b$ phase space)

With the presented binning, **uncertainties range between 10-30%**

With the full Run-2 dataset in our hands, we can more accurately start to probe these differential measurements!

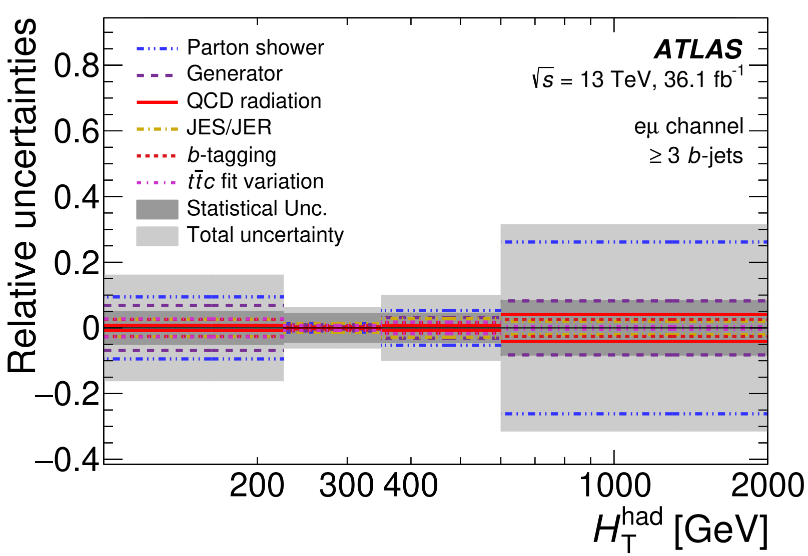

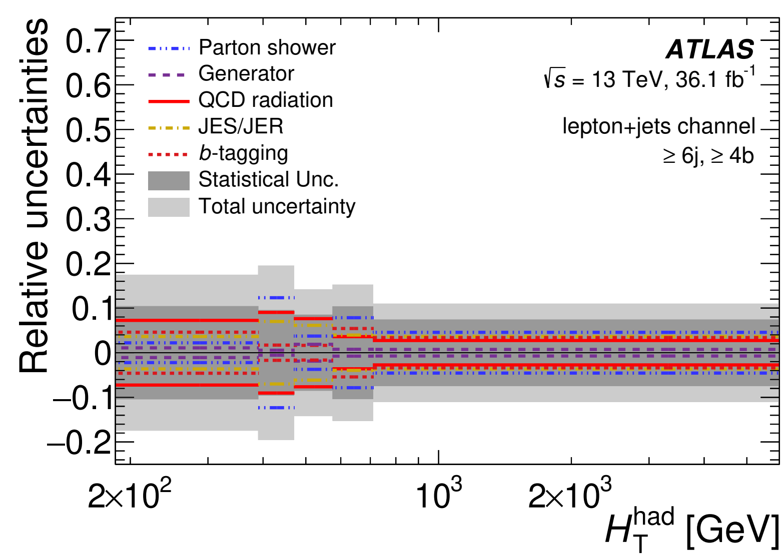

Jet-parton matching

Event kinematics + jet flavour as input to a neural network (NN)

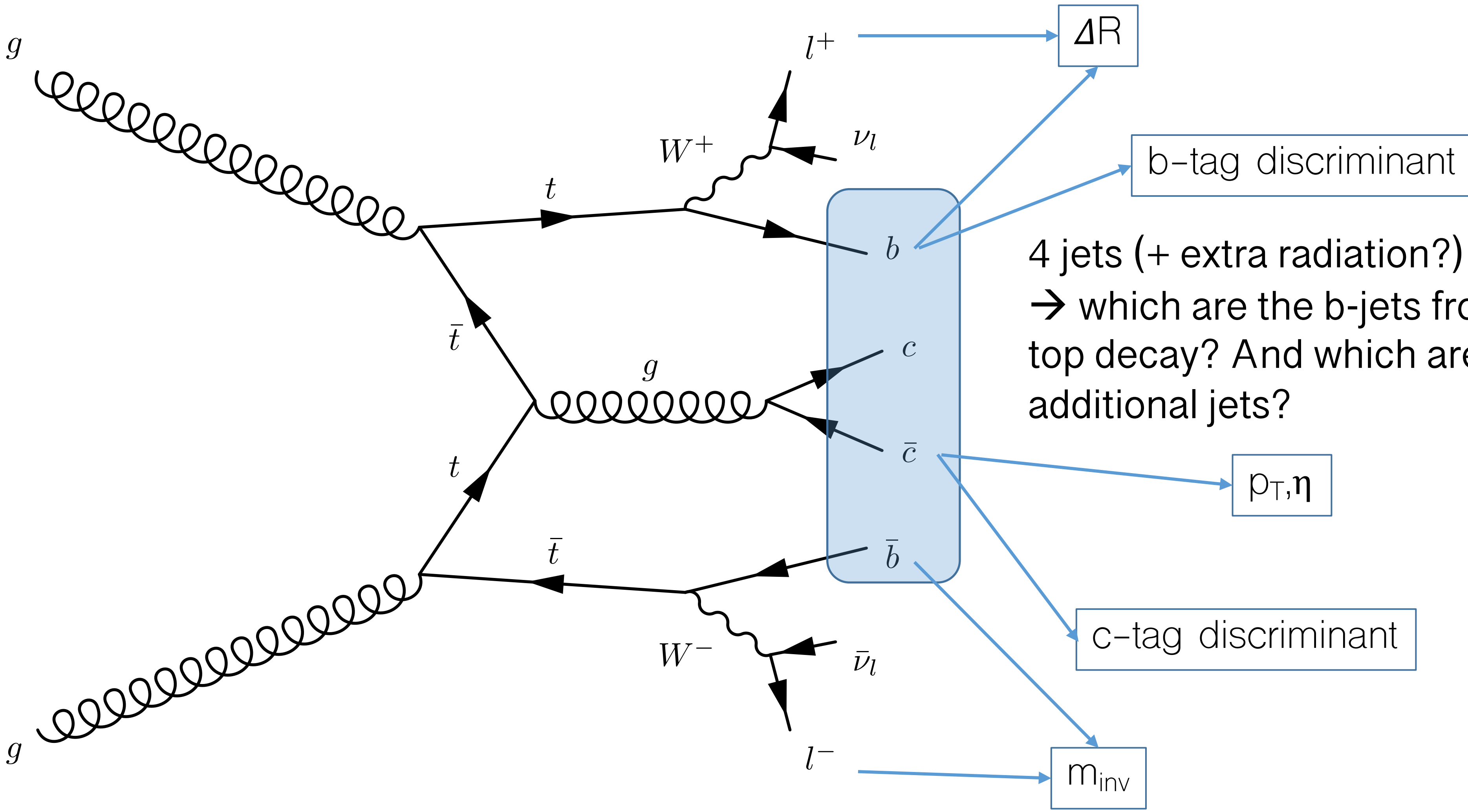

4 jets (+ extra radiation?)
→ which are the b-jets from the top decay? And which are the additional jets?

→ Combine in a NN and pick the best jet-parton assignment

Only ~ 76% of events have two b jets matched to two gen-level b quarks from top quark within $\Delta R<0.3$. Only these are used in the training of the NN.

The network correctly identifies the two additional c (b) jets in **50% (30%)** of the cases for $t\bar{t}c\bar{c}$ ($t\bar{t}b\bar{b}$) events.

Good agreement between the data (black markers) and the simulation (filled histograms).

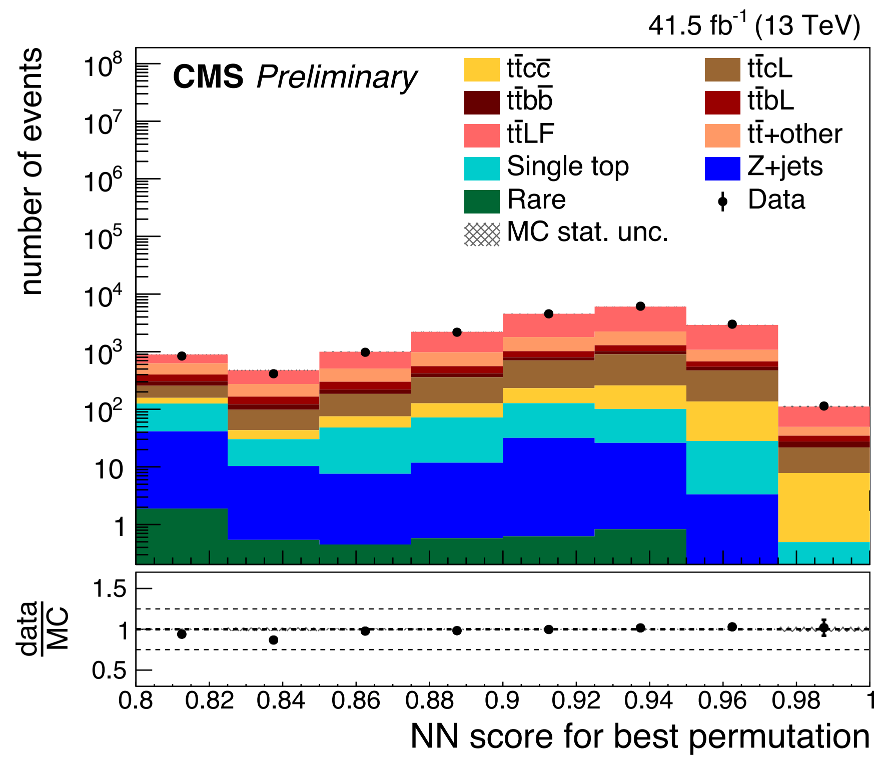

Two hidden layers that comprise 50 neurons each, with ReLu activation functions and a 10% dropout

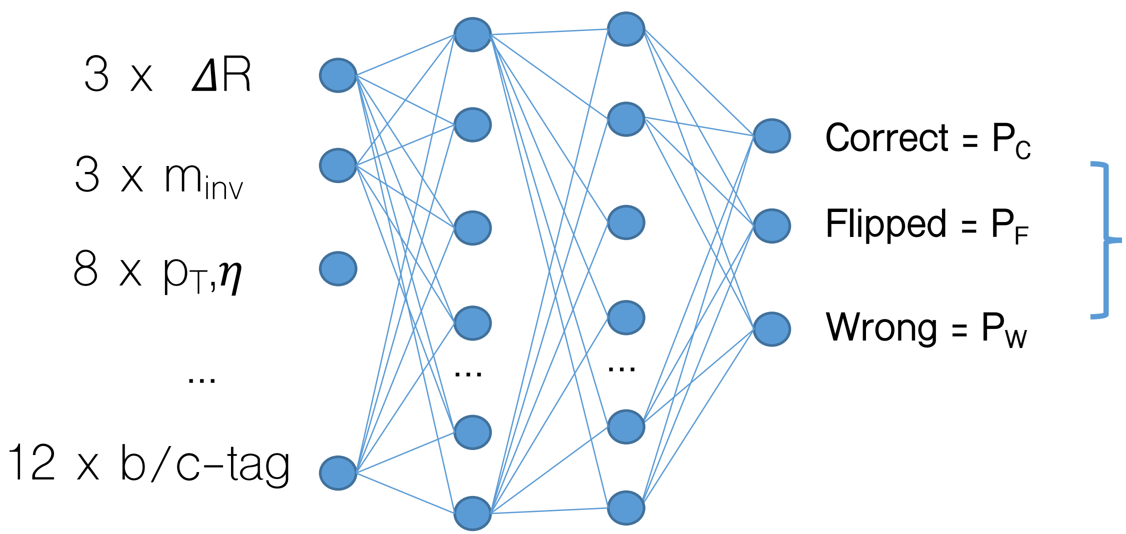

NN score for best permutation

$$= \max\left(\frac{P_C}{P_C+P_W}\,,\,\frac{P_F}{P_F+P_W}\right)$$

JINST 13 (2018) P05011

The DeepCSV heavy-flavour tagging algorithm is a multi-class algorithm that predicts probabilities (P) for jets to originate from a b, c or light-flavour (udsg) quark (or gluon).

This discrimination is based on properties such as track displacement, secondary vertex mass/flight distance, …

Properties from c jets are distributed midway between those of b or light-flavour jets → two c-tagging discriminants!

$$\mathrm{P(CvsL)} = \frac{\mathrm{P(c)}}{\mathrm{P(c) + P(udsg)}}, \qquad \mathrm{P(CvsB)} = \frac{\mathrm{P(c)}}{\mathrm{P(c) + P(b) + P(bb)}}.$$

To use these discriminants in a neural network, the 2-dim shape in simulations needs to be calibrated to the data!

Novel shape calibration of the two-dimensional CvsL and CvsB DeepCSV c-tagger discriminators

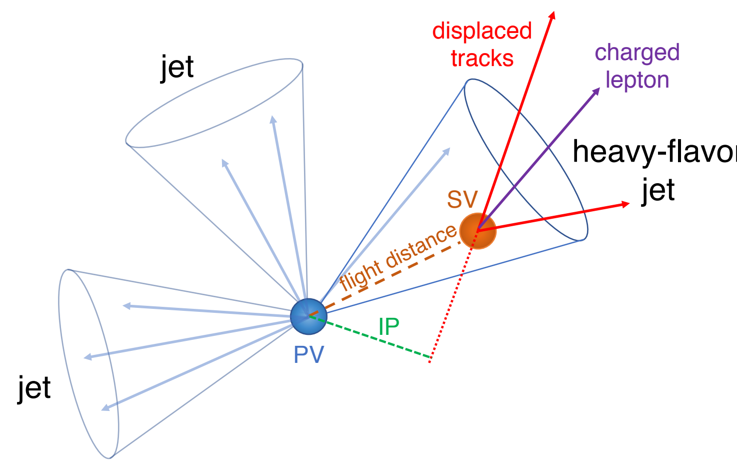

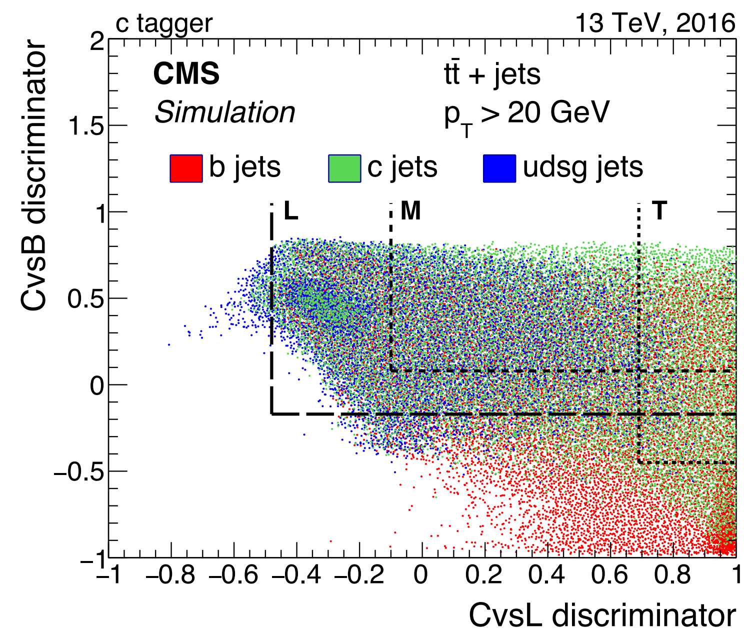

Three control regions for flavor enrichment

W+charm	semi-leptonic $t\bar{t}$	DY + jets
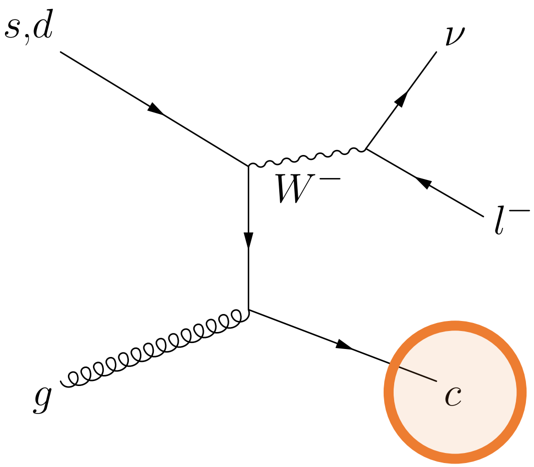	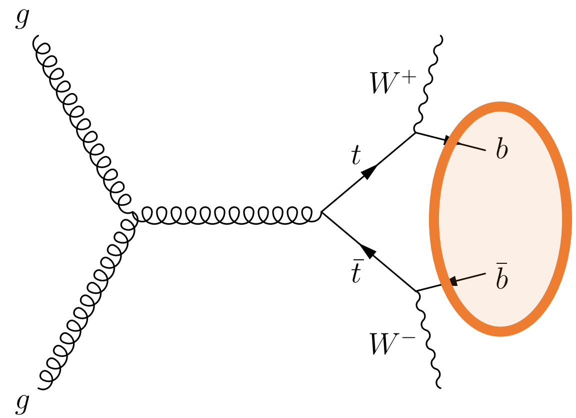	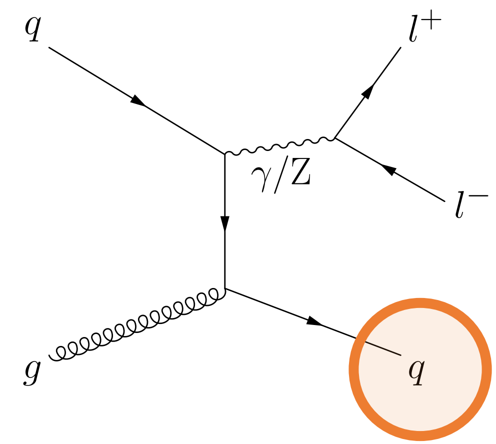
c-enriched (93% pure) (after OS-SS subtraction)	b-enriched (81% pure)	light-enriched (86% pure)

Very good purity in different control regions!

Iterative fitting procedure per (2-dim.) bin, by iterating multiple times over the three control regions → 2-dim SF maps i.e. SF(CvsL, CvsB, flavour)

Template fit using NN discriminator

Defining the neural network

one hidden layer that comprises 30 neurons with
ReLu activation functions and a 10% dropout

CvsL add. jet 1

CvsL add. jet 2

CvsB add. jet 1

CvsB add. jet 2

Parton match NN

ΔR(add. Jets)

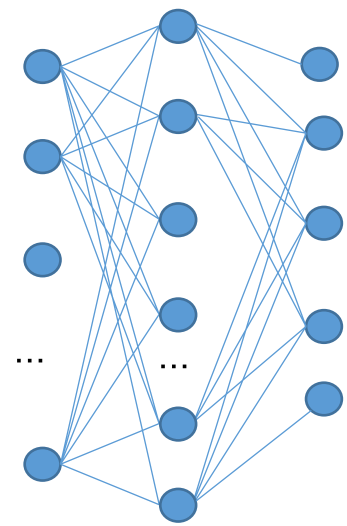

$\mathrm{P}(t\bar{t}c\bar{c})$

$\mathrm{P}(t\bar{t}c\mathrm{L})$

$\mathrm{P}(t\bar{t}b\bar{b})$

$\mathrm{P}(t\bar{t}b\mathrm{L})$

$\mathrm{P}(t\bar{t}\mathrm{LF})$

$$\Delta_b^c = \frac{\mathrm{P}(t\bar{t}c\bar{c})}{\mathrm{P}(t\bar{t}c\bar{c}) + \mathrm{P}(t\bar{t}b\bar{b})}$$

$$\Delta_L^c = \frac{\mathrm{P}(t\bar{t}c\bar{c})}{\mathrm{P}(t\bar{t}c\bar{c}) + \mathrm{P}(t\bar{t}\mathrm{LF})}$$

Δ_b^c and Δ_L^c can be interpreted as topology-specific c-tagger discriminants

Information on the flavour of the two additional jets

Additional information on the event kinematics to most optimally distinguish different signal categories

Results

Comparison between the prefit and the postfit distributions

Two-dimensional distributions are unrolled onto a one-dimensional histogram
4x4 binning results in 16 bins with varying flavor composition:

$$\Delta_L^c \otimes \Delta_b^c : [0, 0.45, 0.6, 0.9, 1.0] \otimes [0, 0.3, 0.45, 0.5, 1.0]$$

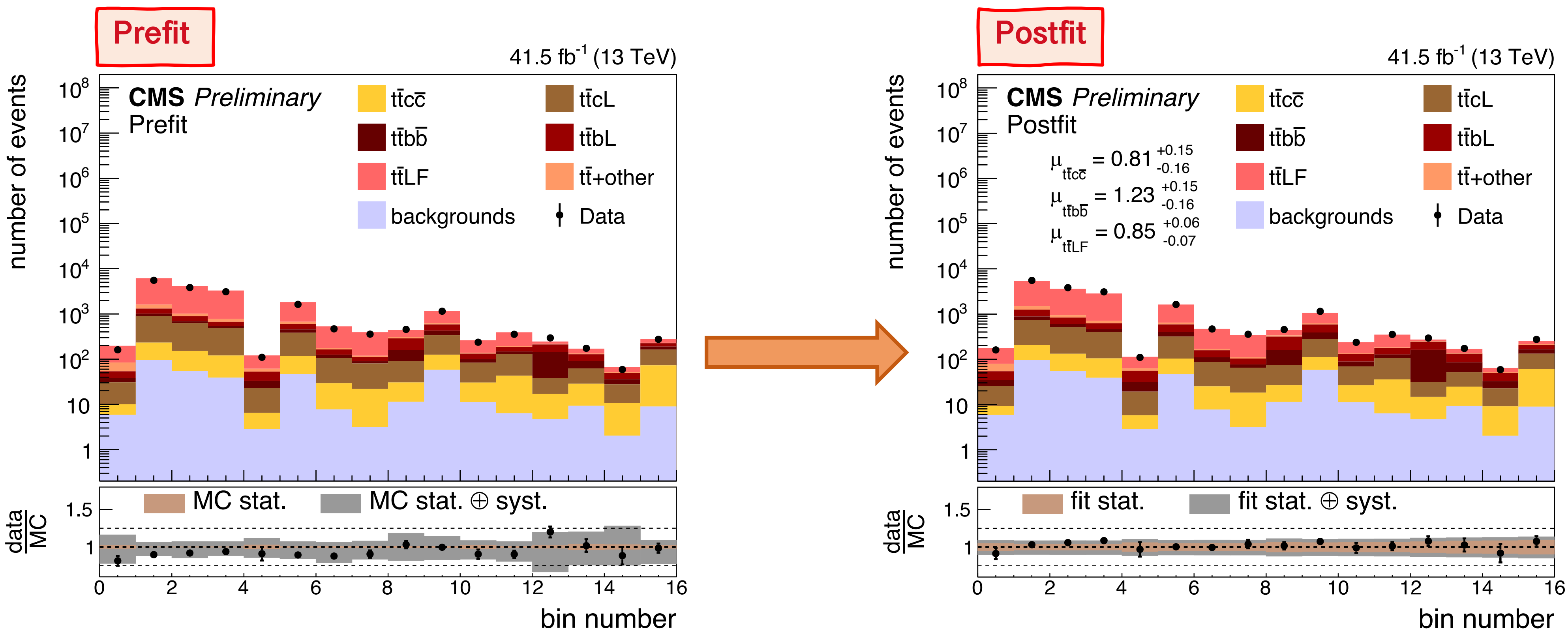

μ represent the signal strength, related to the cross section: $\sigma = \frac{\mu \times N^{MC}}{\mathcal{L}^{int} \times \epsilon}$

Results

Inclusive cross sections in the fiducial phase space

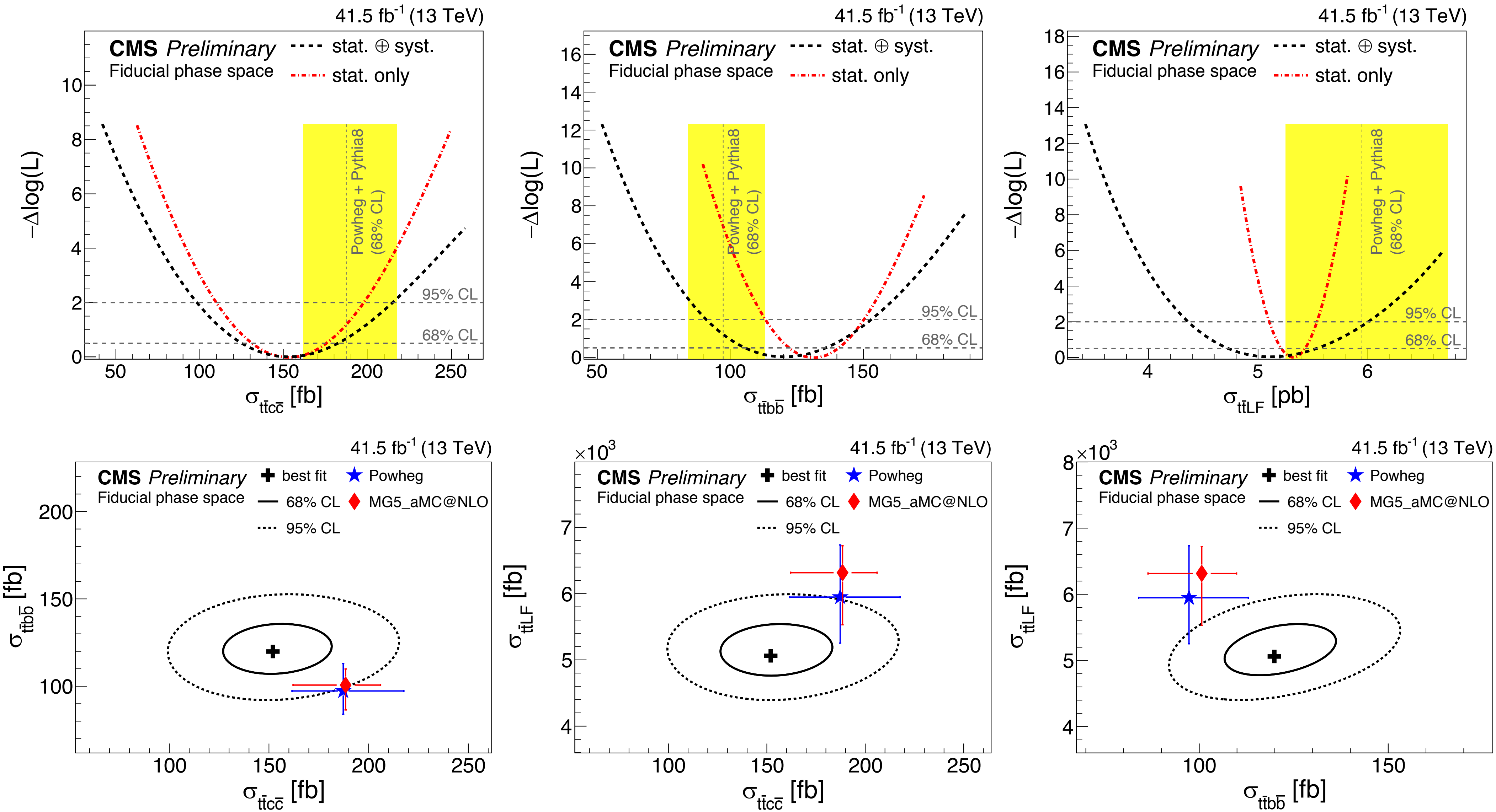

Some tension observed, but overall agreement within 1-2 standard deviations

→measured $t\bar{t}b\bar{b}$ ($t\bar{t}c\bar{c}$ and $t\bar{t}LF$) cross section higher (lower) than predicted.

Ratios R_c and R_b in the fiducial phase space

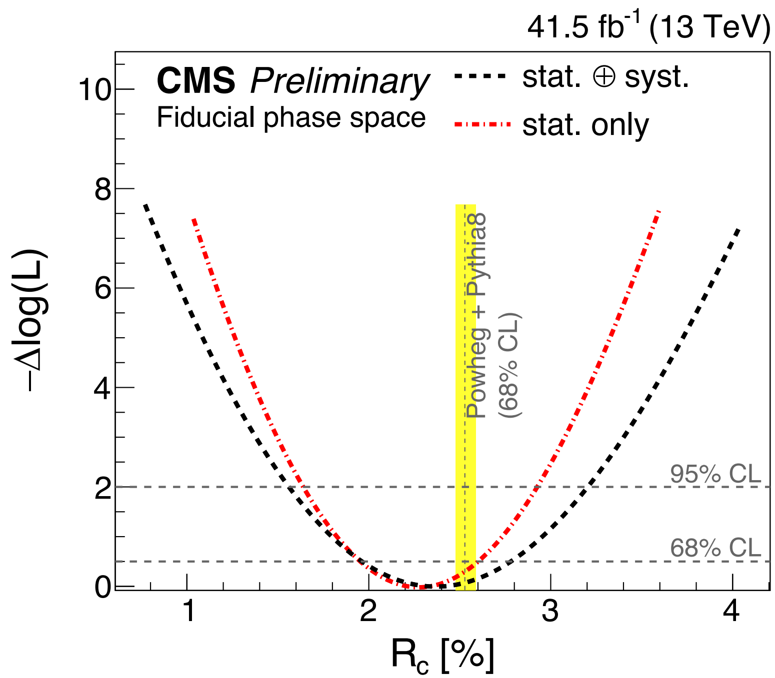

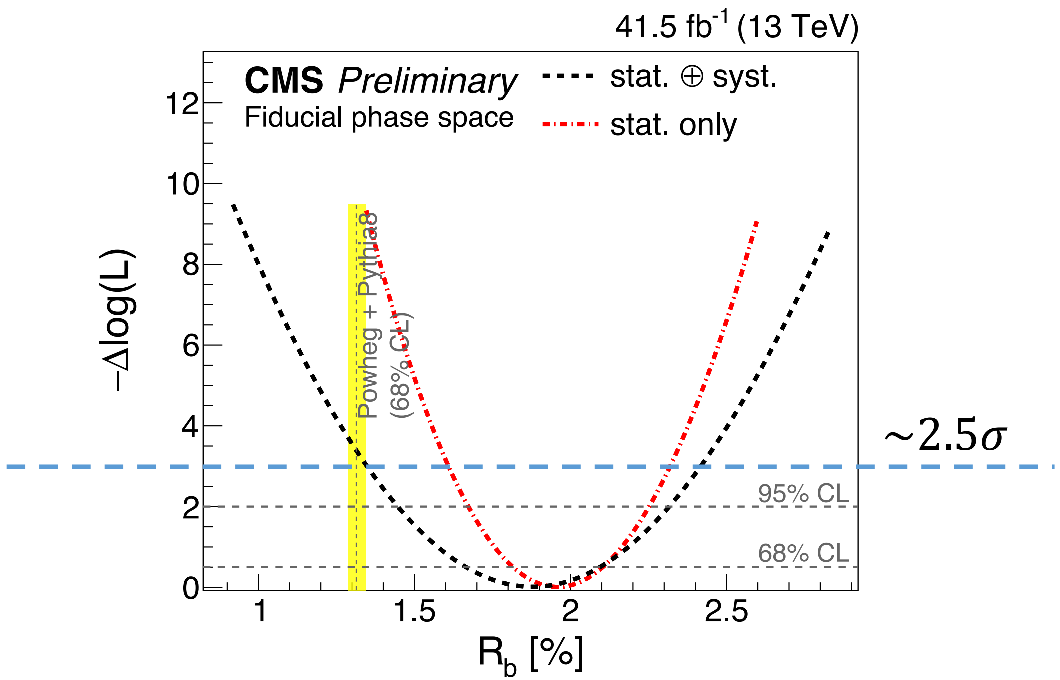

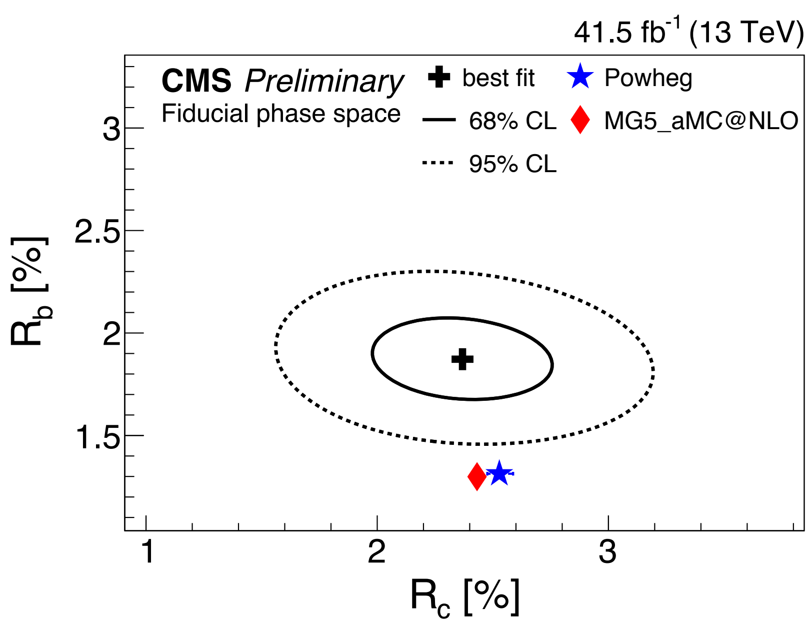

R_c is in very good agreement with theory prediction.

Largest tension observed for R_b

$-\Delta \log L \sim 3 \rightarrow \sim 2.5\sigma$

Numerical values + extrapolation to the full phase space

	Result	Uncertainty	POWHEG	MG5_AMC@NLO	
Fiducial phase space					
$\sigma_{t\bar{t}c\bar{c}}$ [pb]	0.152	$\pm$ 0.022 (stat.) $\pm$ 0.019 (syst.)	0.187 $\pm$ 0.030	0.188 $\pm$ 0.026	~19 %
$\sigma_{t\bar{t}b\bar{b}}$ [pb]	0.120	$\pm$ 0.009 (stat.) $\pm$ 0.012 (syst.)	0.097 $\pm$ 0.016	0.101 $\pm$ 0.014	
$\sigma_{t\bar{t}LF}$ [pb]	5.06	$\pm$ 0.11 (stat.) $\pm$ 0.41 (syst.)	5.95 $\pm$ 0.79	6.32 $\pm$ 0.79	
R_c [%]	2.37	$\pm$ 0.32 (stat.) $\pm$ 0.25 (syst.)	2.53 $\pm$ 0.06	2.43 $\pm$ 0.06	~17 %
R_b [%]	1.87	$\pm$ 0.14 (stat.) $\pm$ 0.16 (syst.)	1.31 $\pm$ 0.03	1.30 $\pm$ 0.03	
Full phase space					
$\sigma_{t\bar{t}c\bar{c}}$ [pb]	7.43	$\pm$ 1.07 (stat.) $\pm$ 0.95 (syst.)	9.15 $\pm$ 1.44	8.92 $\pm$ 1.26	
$\sigma_{t\bar{t}b\bar{b}}$ [pb]	4.12	$\pm$ 0.32 (stat.) $\pm$ 0.42 (syst.)	3.35 $\pm$ 0.54	3.39 $\pm$ 0.49	
$\sigma_{t\bar{t}LF}$ [pb]	217.0	$\pm$ 4.6 (stat.) $\pm$ 18.1 (syst.)	255.1 $\pm$ 32.0	260.6 $\pm$ 32.8	
R_c [%]	2.64	$\pm$ 0.36 (stat.) $\pm$ 0.28 (syst.)	2.82 $\pm$ 0.07	2.72 $\pm$ 0.05	
R_b [%]	1.47	$\pm$ 0.11 (stat.) $\pm$ 0.13 (syst.)	1.03 $\pm$ 0.03	1.03 $\pm$ 0.02	

Results

Comparison to other ttbb analyses

	Result	Uncertainty	POWHEG	MG5_AMC@NLO
Fiducial phase space				
$\sigma_{t\bar{t}c\bar{c}}$ [pb]	0.152	$\pm$ 0.022 (stat.) $\pm$ 0.019 (syst.)	0.187 $\pm$ 0.030	0.188 $\pm$ 0.026
$\sigma_{t\bar{t}b\bar{b}}$ [pb]	0.120	$\pm$ 0.009 (stat.) $\pm$ 0.012 (syst.)	0.097 $\pm$ 0.016	0.101 $\pm$ 0.014
$\sigma_{t\bar{t}LF}$ [pb]	5.06	$\pm$ 0.11 (stat.) $\pm$ 0.41 (syst.)	5.95 $\pm$ 0.79	6.32 $\pm$ 0.79
R_c [%]	2.37	$\pm$ 0.32 (stat.) $\pm$ 0.25 (syst.)	2.53 $\pm$ 0.06	2.43 $\pm$ 0.06
R_b [%]	1.87	$\pm$ 0.14 (stat.) $\pm$ 0.16 (syst.)	1.31 $\pm$ 0.03	1.30 $\pm$ 0.03
Full phase space				
$\sigma_{t\bar{t}c\bar{c}}$ [pb]	7.43	$\pm$ 1.07 (stat.) $\pm$ 0.95 (syst.)	9.15 $\pm$ 1.44	8.92 $\pm$ 1.26
$\sigma_{t\bar{t}b\bar{b}}$ [pb]	4.12	$\pm$ 0.32 (stat.) $\pm$ 0.42 (syst.)	3.35 $\pm$ 0.54	3.39 $\pm$ 0.49
$\sigma_{t\bar{t}LF}$ [pb]	217.0	$\pm$ 4.6 (stat.) $\pm$ 18.1 (syst.)	255.1 $\pm$ 32.0	260.6 $\pm$ 32.8
R_c [%]	2.64	$\pm$ 0.36 (stat.) $\pm$ 0.28 (syst.)	2.82 $\pm$ 0.07	2.72 $\pm$ 0.05
R_b [%]	1.47	$\pm$ 0.11 (stat.) $\pm$ 0.13 (syst.)	1.03 $\pm$ 0.03	1.03 $\pm$ 0.02

PAS-TOP-20-003

$+2.5\sigma$

TOP-18-002	$R_{t\bar{t}b\bar{b}/t\bar{t}jj}$	$\sigma_{t\bar{t}jj}$ [pb]	$\sigma_{t\bar{t}b\bar{b}}$ [pb]
	Dilepton channel (VPS)		
POWHEG + PYTHIA8	0.013 ± 0.002	2.41 ± 0.21	0.032 ± 0.004
Measurement	$0.017 \pm 0.001 \pm 0.001$	$2.36 \pm 0.02 \pm 0.20$	$0.040 \pm 0.002 \pm 0.005$
	Dilepton channel (FPS)		
POWHEG + PYTHIA8	0.014 ± 0.003	163 ± 21	2.3 ± 0.4
MG_aMC@NLO + PYTHIA8 5FS [FxFx]	0.015 ± 0.003	159 ± 25	2.4 ± 0.4
POWHEG + HERWIG++	0.011 ± 0.002	170 ± 25	1.9 ± 0.3
Measurement	$0.018 \pm 0.001 \pm 0.002$	$159 \pm 1 \pm 15$	$2.9 \pm 0.1 \pm 0.5$
	Lepton+jets channel (VPS)		
POWHEG + PYTHIA8	0.017 ± 0.002	30.5 ± 3.0	0.52 ± 0.06
Measurement	$0.020 \pm 0.001 \pm 0.001$	$31.0 \pm 0.2 \pm 2.9$	$0.62 \pm 0.03 \pm 0.07$
	Lepton+jets channel (FPS)		
POWHEG + PYTHIA8	0.013 ± 0.002	290 ± 29	3.9 ± 0.4
MG_aMC@NLO + PYTHIA8 5FS [FxFx]	0.014 ± 0.003	280 ± 40	4.1 ± 0.4
POWHEG + HERWIG++	0.011 ± 0.002	321 ± 36	3.4 ± 0.5
Measurement	$0.016 \pm 0.001 \pm 0.001$	$292 \pm 1 \pm 29$	$4.7 \pm 0.2 \pm 0.6$

$+1.8\sigma$

30 GeV

$+2.1\sigma$

TOP-18-011	Fiducial, parton-independent (pb)	Fiducial, parton-based (pb)	Total (pb)
Measurement	$1.6 \pm 0.1^{+0.5}_{-0.4}$	$1.6 \pm 0.1^{+0.5}_{-0.4}$	$5.5 \pm 0.3^{+1.6}_{-1.3}$
POWHEG ($t\bar{t}$)	1.1 ± 0.2	1.0 ± 0.2	3.5 ± 0.6
POWHEG ($t\bar{t}$) + HERWIG++	0.8 ± 0.2	0.8 ± 0.2	3.0 ± 0.5
MADGRAPH5_aMC@NLO (4FS $t\bar{t}b\bar{b}$)	0.8 ± 0.2	0.8 ± 0.2	2.3 ± 0.7
MADGRAPH5_aMC@NLO (5FS $t\bar{t}$+jets, FxFx)	1.0 ± 0.1	1.0 ± 0.1	3.6 ± 0.3

TOP-16-010

Phase space		$\sigma_{t\bar{t}b\bar{b}}$ [pb]	$\sigma_{t\bar{t}jj}$ [pb]	$\sigma_{t\bar{t}b\bar{b}}/\sigma_{t\bar{t}jj}$
Visible	Measurement	0.088 $\pm$ 0.012 $\pm$ 0.029	3.7 $\pm$ 0.1 $\pm$ 0.7	0.024 $\pm$ 0.003 $\pm$ 0.007
	SM (POWHEG)	0.070 $\pm$ 0.009	5.1 $\pm$ 0.5	0.014 $\pm$ 0.001
Full	Measurement	4.0 $\pm$ 0.6 $\pm$ 1.3	184 $\pm$ 6 $\pm$ 33	0.022 $\pm$ 0.003 $\pm$ 0.006
	SM (POWHEG)	3.2 $\pm$ 0.4	257 $\pm$ 26	0.012 $\pm$ 0.001

$+1.5\sigma$